Tectonophysics 700–701 (2017) 60–79

Contents lists available at ScienceDirect

Tectonophysics

journal homepage: www.elsevier.com/locate/tecto

First records of *syn*-diagenetic non-tectonic folding in quaternary thermogene travertines caused by hydrothermal incremental veining

Andrea Billi [a,*], Gabriele Berardi [b], Jean-Pierre Gratier [c], Federico Rossetti [b], Gianluca Vignaroli [a], M. Oruç Baykara [d,e], Stefano M. Bernasconi [f], Sándor Kele [g], Michele Soligo [b], Luigi De Filippis [h], Chuan-Chou Shen [d]

[a] Consiglio Nazionale delle Ricerche, IGAG, Rome, Italy
[b] Dipartimento di Scienze, Università Roma Tre, Italy
[c] ISTerre, Université Grenoble Alpes and CNRS, 38041 Grenoble, France
[d] High-Precision Mass Spectrometry and Environment Change Laboratory (HISPEC), Department of Geosciences, National Taiwan University, Taipei, Taiwan ROC
[e] Pamukkale University, Department of Geological Engineering, Denizli, Turkey
[f] Geologisches Institut, ETH Zürich, Switzerland
[g] Institute for Geological and Geochemical Research, Research Centre for Astronomy and Earth Sciences, Hungarian Academy of Sciences, Budapest, Hungary
[h] Liceo Scientifico Statale 'L. Spallanzani', Tivoli, Italy

ARTICLE INFO

Article history:
Received 16 July 2016
Received in revised form 8 February 2017
Accepted 14 February 2017
Available online 16 February 2017

Keywords:
Fold
Vein
Buckling
Hydrothermalism
Crystallization force
Quaternary

ABSTRACT

This study is the first documentation of *syn*-diagenetic non-tectonic contractional deformations observed in two Pleistocene thermogene travertine deposits from the late Miocene-Pleistocene Tuscan extensional-hydrothermal province (Italy). The deposits consist of primary porous beds hosting secondary bed-parallel carbonate veins. The porous beds are generally flat-lying, particularly in the upper section of the deposits, whereas the veined beds frequently form undulated structures. These structures are up to a few meters in wavelength, are mostly confined within the lower-middle section of the deposits, and are here mostly interpreted as folds. Field observations, U-Th geochronology, and stable isotope analyses are used to characterize the origin of veins and folds. Radiometrically-determined age inversions, structure overprinting relationships, downward growth of vein crystals, deformation of primary sedimentary structures, and downward increasing frequency of veins and folds show that the undulated travertine beds can be mainly interpreted as the product of *syn*-diagenetic hydrothermal rejuvenation causing non-tectonic veining and folding. The non-tectonic hypothesis is also supported by the absence of contractional deformation in the travertine-hosting sediments. The folds were generated by complex mechanisms including bending and buckling caused by laterally-confined volume expansion during *syn*-diagenetic circulation of mineralizing fluids and related incremental veining. Modeling some folds with the Biot-Ramberg's buckling equation shows a vein-to-host travertine viscosity ratio between 1.5 and 4, confirming the *syn*-diagenetic origin of folds. Veining and folding changed some original properties of travertines including rheology, fabric, porosity, and chronological sequence. The identification of these structures and related changes of rock properties (e.g., age rejuvenation) is relevant for the proper interpretation of thermogene travertines as recorders of many geological processes including paleoclimate oscillations, earthquake occurrences, hydrothermal circulations, and uplift or incision rates. Synthesizing, the studied thermogene travertines appear more like sedimentary-hydrothermal-hybrid zoned deposits rather than pure sedimentary systems uniquely responding to the superposition law.

1. Introduction

Owing to their chemical nature and good datability through U-Th methods (Crossey et al., 2006; Uysal et al., 2007; Shen et al., 2012), Quaternary thermogene travertines are increasingly being used as fundamental records of many geological processes and parameters including climate oscillations (Rihs et al., 2000; Wang et al., 2004, 2014; Faccenna et al., 2008; De Filippis et al., 2013b), earthquake occurrences (Tuccimei et al., 2006; Piper et al., 2007; Uysal et al., 2009; Ünal-İmer et al., 2016), fault slip rates (Pederson et al., 2013; Ricketts et al., 2014), fracture/vein opening rates (Uysal et al., 2007; Gratier et al., 2012), uplift and/or river incision rates (Crossey and Karlstrom, 2012; Crossey et al., 2015; Karlstrom et al., 2017), hydrological-hydrothermal circulations (Crossey et al., 2009; Priewisch et al., 2014), parental fluid

* Corresponding author at: Consiglio Nazionale delle Ricerche, IGAG, c.o. Dipartimento Scienze della Terra, Sapienza Università di Roma, P.le A. Moro 5, 00185 Rome, Italy.
E-mail address: andrea.billi@cnr.it (A. Billi).

http://dx.doi.org/10.1016/j.tecto.2017.02.014
0040-1951/

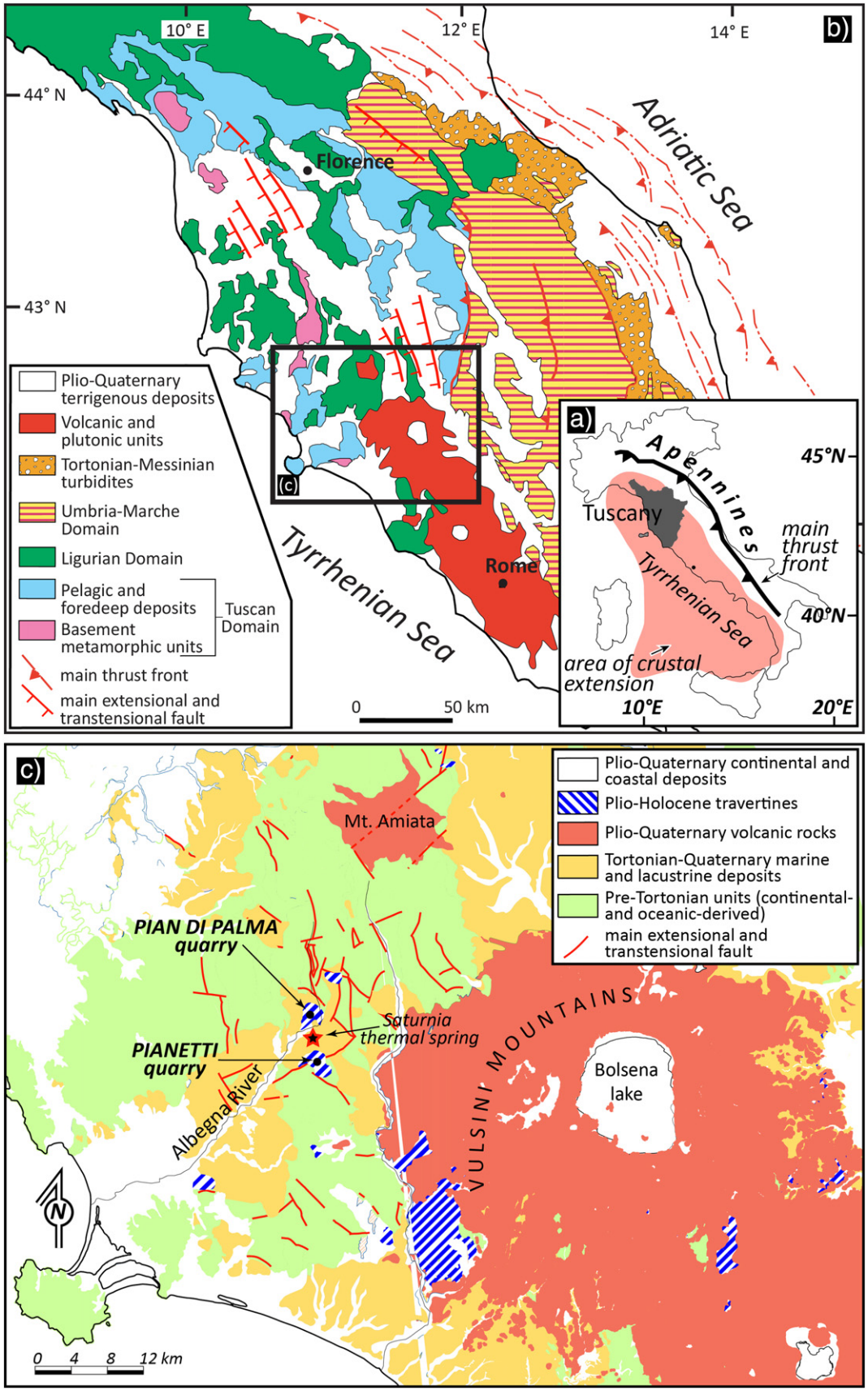

Fig. 1. Geological setting. (a) Location of the study area (Albegna basin in Tuscany) in central Italy along the Tyrrhenian Sea basin. (b) Geological map of Tuscany and central-northern Apennines. (c) Geological map of the upper Albegna basin, where the studied Pianetti and Pian di Palma travertine deposits are located. Coordinates of the two study quarries are as follows: Pianetti quarry, 42°37′59.69″N, 11°30′39.76″E; Pian di Palma quarry, 42°41′21.11″N, 11°29′52.88″E.

Fig. 2. Investigated sites. (a) Panoramic view of the travertine deposit exposed in the Pianetti quarry. (b) Close-up photograph from the Pianetti quarry showing the transition from vein-dominated folded (below) and non-veined flat host (above) travertines. (c) Panoramic view of the travertine deposit exposed in the Pian di Palma quarry. The Pian di Palma travertine is characterized by a depositional architecture very similar to that of the Pianetti travertine. (d) Close-up photograph from the Pian di Palma quarry showing the transition from vein-dominated folded (below) and non-veined flat host (above) travertines.

temperatures (Kele et al., 2015), mantle degassing (Crossey et al., 2016; Ring et al., 2016; Sinisi et al., 2016), CO_2 leakage rates (Shipton et al., 2004; Dockrill and Shipton, 2010; Kampman et al., 2012; Burnside et al., 2013; Karlstrom et al., 2013; Frery et al., 2015, 2016; Berardi et al., 2016), and also age of fossil hominids (Lebatard et al., 2014). Moreover, subsalt travertine-like porous rocks along the Atlantic Brazilian and Angolan margins have been recently discovered to be reservoirs of major hydrocarbon reserves (Beasley et al., 2010). Therefore, understanding the complete history of deposition and diagenetic deformation/alteration of travertines as well as identifying the occurrence of possible post-deposition rejuvenation events is the essential prerequisite to properly sample and analyze these rocks with the aim of temporally and spatially unraveling some geological processes and parameters as mentioned above. Also, the relevance as hydrocarbon reservoirs imposes a better understanding and identification of travertine diagenetic processes and related changes of rock properties (e.g., primary porosity vs. secondary cementation; Ronchi and Cruciani, 2015; Soete et al., 2015; Claes et al., 2016; Rodríguez-Berriguete et al., 2016).

Focusing on the diagenetic alteration, we aim at responding to three main questions: (1) what happens to the freshly deposited porous travertines with a continuous *syn*-diagenetic supply of mineralizing fluids? (2) Can this fluid alter and rejuvenate the primary travertine modifying some of its original properties such as fabric, porosity, chronological sequence, and rheology? (3) Can diagenesis and possible rejuvenation influence or even compromise travertine-based Quaternary geological reconstructions and interpretations?

Using a multidisciplinary approach that combines field observations, U-Th geochronology, and stable isotope analyses, we address these questions analyzing two deposits of Pleistocene thermogene travertine from southern Tuscany, central Italy (Fig. 1). We provide, in particular, the first records of *syn*-diagenetic non-tectonic folding of thermogene travertines caused by laterally-confined volume expansion through hydrothermal incremental veining, with related changes of rock properties such as porosity reduction, rock strengthening, and age rejuvenation. The occurrence of similar structures in other thermogene travertine deposits as well as in other sedimentary (and/or diagenetic) environments corroborates the relevance of our results and suggests that structures similar to those reported in this paper may be more common than previously thought and may be relevant for other sedimentary rocks. We show that some structures that we interpret as *syn*-diagenetic folds are very similar to structures that in other travertine deposits are interpreted as depositional features. Although we do not aim to resolve this dispute, our work has a twofold purpose: (1) opening a debate over the occurrence and significance of primary vs. secondary (*syn*-diagenetic) structures in thermogene travertines and (2) defining a set of geological criteria suitable to discriminate primary from secondary structures. If unrecognized, secondary travertine structures could potentially lead to misinterpretations of travertine-based spatio-temporal geological reconstructions. We believe that our *syn*-diagenetic deformation and rejuvenation model has the potential to profoundly influence the current understanding of thermogene travertines and related geological interpretations. We will indeed demonstrate that the two studied thermogene travertine deposits are, for some features, partially closer to hydrothermal/alteration zoned ore-like deposits (e.g., Gresens, 1967; Browne, 1978; Rose and Burt, 1979; Giggenbach, 1992; Einaudi et al., 2003; Rae et al., 2003; Simmons and Graham, 2003; Rossetti et al., 2007; Shanks, 2012; Vignaroli et al., 2015; Eide et al., 2017) rather than to primary pure carbonate sedimentary systems uniquely responding to the superposition law (e.g., Guo and Riding, 1994, 1998; Gandin and Capezzuoli, 2008). We will thus propose that thermogene travertines should be examined and interpreted with more caution as geochemical and temporal markers.

2. Geological setting

The studied deposits are located and excellently exposed in the Pianetti and Pian di Palma quarries (Fig. 2) within the late Miocene-Pleistocene Albegna extensional basin, southern Tuscany. This region is located in the hinterland (west) of the Paleogene-Quaternary northern Apennines fold-thrust belt in central Italy (Fig. 1), which developed through an eastward migration of thrust fronts and foredeep basins in a classical piggy-back sequence toward the Adriatic foreland (e.g., Patacca et al., 1990; Cipollari and Cosentino, 1995; Billi et al., 2006; Billi and Tiberti, 2009; Brogi et al., 2015; Beaudoin et al., 2016; Brogi, 2016). During Neogene and Quaternary times, at the rear (west) of the Apennines fold-thrust belt, a post-orogenic extensional regime acting all along the Tyrrhenian margin including Tuscany (Malinverno and Ryan, 1986; Faccenna et al., 1997, 2001; Jolivet et al., 1998; Rossetti et al., 1999)

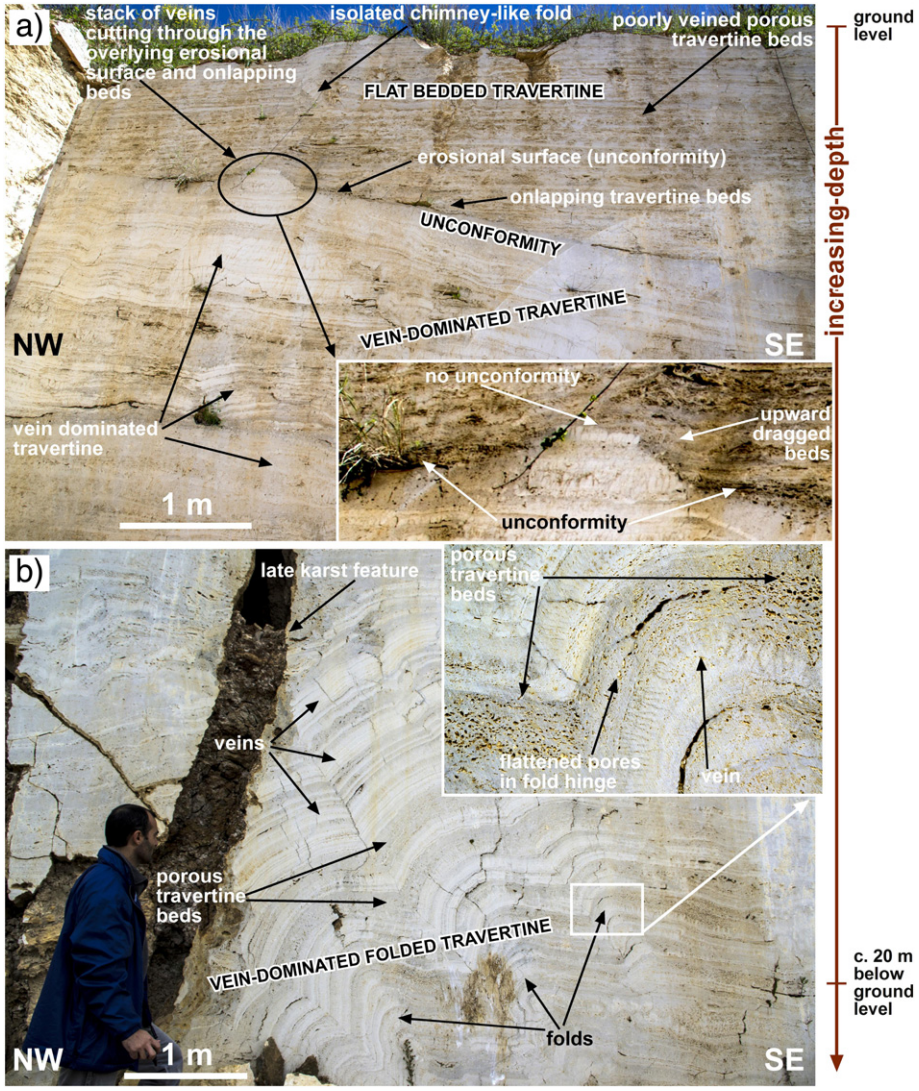

Fig. 3. Photographs of travertine exposures from the Pianetti quarry with increasing depth. (a) Middle and upper section of the Pianetti deposit showing flat porous travertine beds (no or limited veins and folds) onlapping over an erosional surface (unconformity) and the underlying vein-dominated (bed-parallel veins) travertine beds. Note, in the black ellipse, that a stack of bed-parallel sub-horizontal veins cut through, from bottom to top, the overlying erosional horizon (unconformity) and the onlapping travertine beds. Inset (bottom right) shows a close-up photograph of the structure within the ellipse. Note that the vein stack interrupts (i.e., cuts through) the lateral continuity of the southeastward-inclined unconformity that is absent, in contrast, on top of the stack itself. The overlying travertine beds are gently bent upward consistently with the occurrence and upward growth of the vein stack relief. (b) Lower section of the Pianetti deposit showing vein-dominated (bed-parallel veins) folded travertine beds. Inset (top right) displays a close-up photograph showing primary pores (from porous travertine beds) that are progressively flattened and shattered in approaching the fold hinge from the fold limbs. The most important observation is that the pores are not absent in the fold hinge. They are indeed present but strongly flattened as compared with those ones occurring laterally, thus showing the post-depositional deformation of the pores themselves in coincidence with the fold hinge occurrence and development.

led to crustal stretching and formation of wide and deep sedimentary basins usually controlled by NW-striking extensional faults and perpendicular or oblique transtensional transfer zones (Brogi, 2004; Bonciani et al., 2005; Brogi and Fabbrini, 2009; Carmignani et al., 2013; Buttinelli et al., 2014; Liotta et al., 2015; Vignaroli et al., 2016; Conti et al., 2017). The post-orogenic crustal stretching originated also wide magmatic provinces of late Miocene-Quaternary age (Barberi et al., 1971; Innocenti et al., 1992; Serri et al., 1993; Nappi et al., 1995; Rossetti et al., 2007; Cadoux and Pinti, 2009), where endogenic fluid circulation up to the surface occurred and, in places, still occurs mainly along extensional and transtensional faults (Buonasorte et al., 1988; Barberi et al., 1994; Gianelli et al., 1997; Batini et al., 2003; Brogi, 2008; Liotta et al., 2010; Rossetti et al., 2011; Vignaroli et al., 2013, 2016; Berardi et al., 2016; Croci et al., 2016; Rimondi et al., 2015).

In southern Tuscany and nearby peri-Tyrrhenian regions, active and fossil Quaternary travertine deposits occur with variable size and shape often in proximity of the main active or quiescent volcanic districts (e.g., Brogi, 2008; Faccenna et al., 2008; Rimondi et al., 2015; Berardi et al., 2016; Vignaroli et al., 2016). The fossil travertine deposits of the Pianetti and Pian di Palma quarries (Fig. 2) are located within the peri-volcanic rings of the middle-late Pleistocene Amiata (300–190 ka; Cadoux and Pinti, 2009; Laurenzi et al., 2015; Marroni et al., 2015) and Vulsini (590–127 ka; Nappi et al., 1995) volcanic districts, where hydrothermal circulation is still active (e.g., the Saturnia thermal spring; Fig. 1).

The Albegna basin (Fig. 1), which hosts the studied deposits, is a NE-SW-trending extensional tectonic depression filled by late Miocene-Quaternary marine and transitional sediments including clays, sands, gravels, and conglomerates overlain by aeolian sands and fluvial clays and silts. These late Miocene-Quaternary postorogenic sedimentary sequences (Martini and Sagri, 1993; Liotta, 1994; Pascucci et al., 2006; Brogi and Liotta, 2008) unconformably overlie a tectonic nappe stack including, from top to bottom (Carmignani et al., 2013): (i) oceanic-derived units of the Ligurian domain, consisting of marly-arenaceous flysch-type sediments and discontinuous ophiolitic sequences (Lower

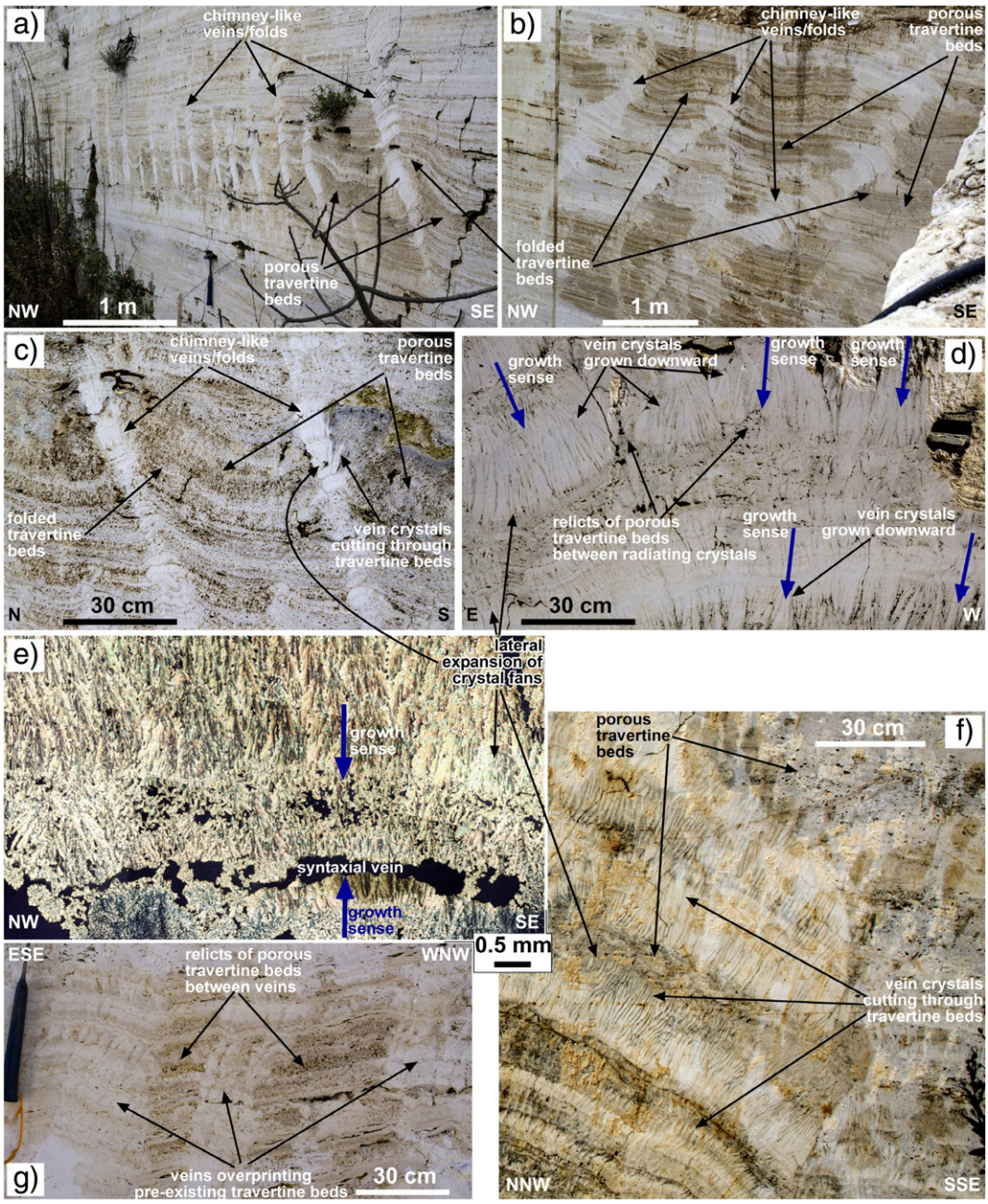

Fig. 4. Photographs of travertine exposures from the Pianetti and Pian di Palma quarries (see also Figs. S1–S39). (a)–(c) Chimney-like folded veins across originally-flat bedded porous travertine (Pian di Palma). (d) Downward growth (blue arrows) of vein radiating crystals, which are perpendicular to bedding and form a bed-parallel gentle anticlinal vein (Pianetti). Note the occurrence of porous travertine relicts between the downward radiating crystals, which grew at the expense of pre-existing travertine beds. (e) Microphotograph (crossed nicols) of a sub-horizontal vein filling characterized by both downward and upward radiating crystals (syntaxial vein; Pianetti). The vein is bed-parallel whereas the crystals and related growth are bed-perpendicular (radiating). In this and other photographs, note the lateral expansion of crystal fans (growth competition), implying a bed-parallel component of growth in addition to the bed-perpendicular one. (f) Alternations of folded veins and porous travertine beds (Pianetti). Note the vein radiating crystals upwardly overprinting the overlying travertine beds, whose relicts are visible between the upward radiating crystals. Also in this case, the veins, which grew at the expense of pre-existing travertine beds, are bed-parallel whereas the crystals and related growth are bed-perpendicular with also a bed-parallel component. (g) Bed-parallel white veins arranged in sub-vertical stacks overprinting and cutting through primary porous beds of travertine (Pianetti). Relicts of porous beds are visible between the white veins.

Fig. 5. Photographs of travertine exposures from the Pianetti and Pian di Palma quarries (see also Figs. S1–S39). (a) Chimney-like stack of bed-parallel veins, which are characterized by a fan-shaped cross-sectional pattern, i.e., the bed-parallel veins are progressively steeper or even overturned downward (Pianetti). Note the occurrence of vein-parallel stylolites (i.e., the stylolite teeth are perpendicular to the vein plane). (b) Chimney-like stack of bed-parallel veins (Pian di Palma). Note the occurrence of vein-parallel stylolites (same as above). (c) Flattening of original travertine pores in fold thickened hinges (Pianetti). Note the presence of post-depositional voids and of a detachment level between folded and flat travertines. (d) Chimney-like stack of bed-parallel veins (Pianetti). In approaching the fold, note the flattening and dragging of primary pores. In this and other photographs, note the lateral expansion of crystal fans, implying a bed-parallel component of growth (growth competition) in addition to the main bed-perpendicular one. (e) Sequence of flat and folded veins (Pian di Palma). Note the occurrence of post-depositional voids and of a detachment level at the transition between flat and folded veins. (f) Travertine folded veins (Pianetti). Note the hinge thickening. (g) Close-up view from the previous photograph. Limb-perpendicular fan-patterned foliations and second-order folds along the upright limb of a travertine anticline. (h), (i) Travertine overturned folds affected in the lower limb by upright small folds resembling refold structures (Pianetti). (j) Bird's eye view of folded veins that are laterally confined by porous bedded travertine (Pian di Palma). The 2D rounded shape of folds in this photograph suggests a 3D domal or botryoidal shape.

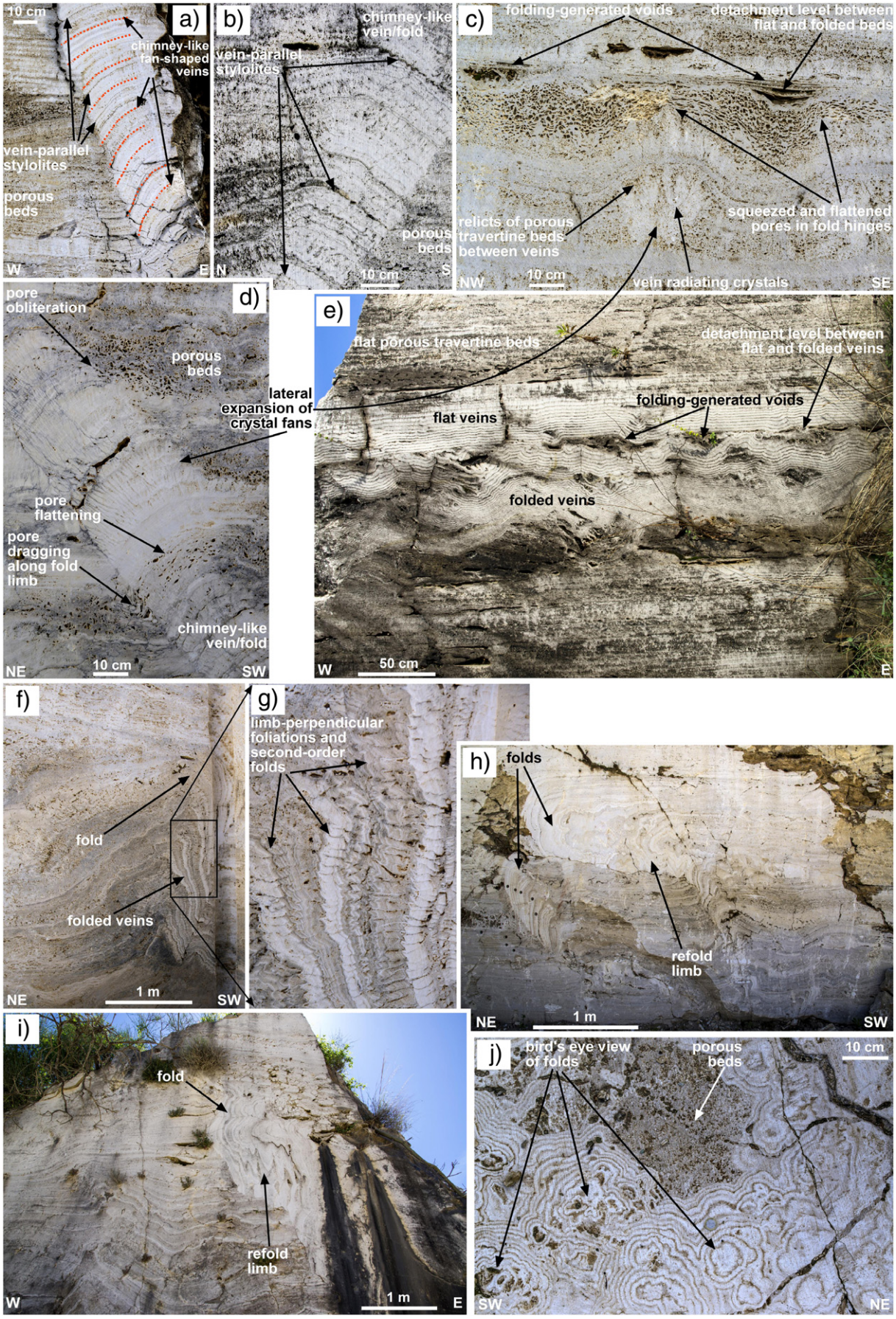
a)
10 cm
chimney-like fan-shaped veins
vein-parallel stylolites
porous beds
W
E
b)
chimney-like vein/fold
vein-parallel stylolites
porous beds
N
S
10 cm
c)
folding-generated voids
detachment level between flat and folded beds
relicts of porous travertine beds between veins
squeezed and flattened pores in fold hinges
vein radiating crystals
NW
SE
10 cm
d)
pore obliteration
porous beds
lateral expansion of crystal fans
pore flattening
pore dragging along fold limb
chimney-like vein/fold
NE
SW
10 cm
e)
flat porous travertine beds
detachment level between flat and folded veins
folding-generated voids
flat veins
folded veins
W
E
50 cm
f)
fold
folded veins
NE
SW
1 m
g)
limb-perpendicular foliations and second-order folds
h)
folds
refold limb
NE
SW
1 m
i)
fold
refold limb
W
E
1 m
j)
bird's eye view of folds
porous beds
10 cm
SW
NE

Cretaceous to Upper Eocene); (ii) continental-derived units of the Tuscan domain consisting of a non-metamorphic succession (Mesozoic carbonates and Cenozoic marly and siliciclastic sedimentary sequences of the Tuscan Nappe) and underlying metamorphic units of the Tuscan Metamorphic Complex. The nappe stack of the Tuscan domain is partly exposed along elongate structural highs bounded by extensional and transtensional faults (e.g., Brogi, 2004; Bonciani et al., 2005; Brogi and Fabbrini, 2009; Carmignani et al., 2013) and partly known from borehole cores drilled mainly for geothermal aims (Buonasorte et al., 1988; Barberi et al., 1994; Batini et al., 2003; Bellani et al., 2004; Bonciani et al., 2005; Rossetti et al., 2008).

The Mesozoic carbonate units of the Tuscan Nappe are particularly relevant for the recent and present geothermal-hydrothermal setting of Tuscany, particularly for the Pliocene-Quaternary thermogene travertine deposits of this region (e.g., Rimondi et al., 2015; Berardi et al., 2016; Vignaroli et al., 2016). At surface and shallow levels, the Mesozoic carbonates have constituted the fractured recharge areas through which meteoric waters have infiltrated to depth. At deeper levels, the same rocks have been the reservoir for meteoric and endogenic fluids, which have mixed before ascending to feed the numerous surface thermal springs and CO_2 emission centers (e.g., Batini et al., 2003; Liotta et al., 2010; Rossetti et al., 2011; Berardi et al., 2016; Vignaroli et al., 2016).

The Pianetti and Pian di Palma travertines (Fig. 2) unconformably lay on top of Neogene-Quaternary sediments of the Albegna basin (Carmignani et al., 2013), which formed under the control of main NE-SW-striking extensional and transtensional faults partly dissecting the basin-filling deposits (Zanchi and Tozzi, 1987; Brogi, 2004; Bellani et al., 2004; Brogi and Fabbrini, 2009). With the exception of the studied travertines (Fig. 2), no folds and other compressional deformations are documented in this basin, at least in the Pliocene-Quaternary sediments that host the studied travertines (Brogi, 2008; Carmignani et al., 2013; Berardi et al., 2016; Vignaroli et al., 2016).

3. Observations and data

3.1. Exposed structures

3.1.1. General features

The Pianetti and Pian di Palma quarries, which are about 6 km apart (Fig. 1c), expose travertines to maximum depths of 25–30 m over up to 200 m wide outcrops (Fig. 2). At the time of our field studies (2013–2015), travertine extraction was active only in the Pianetti quarry (Fig. 2a) while the Pian di Palma quarry (Fig. 2c) was already abandoned since a few years. In both quarries, we recognized two main types of carbonates: (1) primary porous bedded travertines and (2) secondary sparry veins that are bed-parallel and poorly- to non-porous (Fig. 2b and d). In these rocks, Ronchi and Cruciani (2015) measured bulk porosities ranging from less than 3% to ~35% without distinguishing between primary porous travertine and secondary veins. Veins can occur along flat beds but more often occur along undulated beds, which we hereafter call as folds for consistency with our final interpretation of these structures. The main features of veins and folds are described below and shown in Figs. 2–6 and S1–S39. We first provide some preliminary observations on the veins and then we further discuss the crosscutting relationships between veins and folds. We focus, in particular, on the spatial and crosscutting relationships between veins, folds, and host travertine beds to understand the relative timing and mechanism of vein and fold formation.

3.1.2. Veins

Veins are arranged in bed-parallel banded patterns often forming, in two-dimensional views, complex folds (Fig. 3c and d). In many cases, vein crystals can be identified macroscopically (Figs. 4c, d, f, S6–S8, S11–S14, S18, S25, S27, S29, S31, S34, S35, S37, and S38), or under optical microscope magnification (Figs. 4e and S19). These crystals tend to form bed- and vein-normal elongate fan-shaped patterns, which are indicative of the vein growth direction and sense. The growth sense, in particular, is vein-perpendicular from the narrow to the wide portions of crystal blades (Figs. 5c, 5d, 6b, 6f, S7, S8, S14, S18, S19, S25, S31, S34, S35, and S37; e.g., Gratier et al., 2012; Ricketts et al., 2014). However, as these crystals are radiating and therefore laterally-expanding during growth (Figs. 4c–f, 5c, and 5d), a bed-parallel component of expansion (i.e., growth competition sensu Hilgers et al., 2004) is also present besides the bed-normal one. We observed that vein crystals are frequently characterized by a downward radiating pattern, indicating that they grew (inescapably as post-depositional features; e.g., Gratier et al., 2012;) from a pre-existing top travertine bed toward the bottom bed (Figs. 4d, e, 6f, S7, S8, S14, S18, S19, and S25). Under the microscope, it can be observed that these structures can grow also syntaxially along travertine beds with both bed- and vein-normal growth. The crystals can be seen growing and converging toward the center of the vein both from the lower and from the upper travertine beds that form the vein walls (Figs. 4e and S19). Vein crystals often tend to cut through or overprint the pre-existing overlying or underlying bedded porous travertine so that relicts of porous travertine beds can be observed between adjacent radiating vein crystals (Figs. 4c, d, f, g, 5j, S11, S12, S15, S34-S39). Bed-parallel veins formed partly at the expense of (i.e., overprinting) pre-existing porous beds (Figs. 4f, g, 5c, S14, S34–S37) that are more frequent in the upper section of the deposits and fade away downward where veins become prevailing (Fig. 3). An exposure within the Pianetti quarry is particularly illustrative (Fig. 3a). The travertines are characterized by cycles of deposition and non-deposition, the latter being often characterized by erosional horizons (unconformity in Fig. 3a), over which a new cycle of travertine beds can onlap (e.g., Faccenna et al., 2008). In the upper portion of the Pianetti deposit, we observed a stack of bed-parallel sub-horizontal veins cutting, from bottom to top, through an overlying erosional horizon (unconformity) and the onlapping travertine beds (within the black ellipse in Fig. 3a), which are lacking in or are poorly affected by both veins and folds. The crosscutting relationship of Fig. 3(a) indicates that the underlying stack of bed-parallel sub-horizontal veins is younger than both the overlying erosional horizon and the onlapping beds. This evidence is particularly visible on the inset of Fig. 3(a), where the vein stack interrupts (i.e., cutting through) the lateral continuity of the unconformity that is absent on top of the stack itself. Moreover, the overlying travertine beds are gently bent upward consistently with the occurrence and upward growth of the vein stack relief.

3.1.3. Folds

Folds are numerous and mostly restricted to the lower and middle portions of the investigated exposures (Fig. 3b). They range between less than 1 cm and near 10 m in wavelength, and are made of undulated veins or veins alternated with porous travertine beds (Figs. 3b, 4-6, and S1–S39). Folds with various dips of limbs overprint and deform originally flat travertine beds, thus forming structures characterized by various shapes and sizes (Figs. 3b, 4a–c, 5, 6, S5–S18, and S20–S39). In the middle and occasionally in the upper portion of the studied sections, the most frequent folds are discrete sub-vertical chimney-like or columnar

Fig. 6. Photographs of travertine exposures from the Pianetti quarry (see also Figs. S1–S39). (a) Folded veins in the lower portion of the quarry. (b) Close-up view of the previous photograph. Note the limb-perpendicular fan-patterned foliations and second-order folds along the limb of the larger fold visible in the previous photograph. Note also the downward grown crystals of some veins. (c) Folded veins in the lower portion of the quarry. (d) Close-up view of the previous photograph. Note the limb-perpendicular fan-patterned foliations and second-order folds along the limb of the larger anticline visible in the previous photograph. (e) Folded veins in the lower portion of the quarry. (f) Close-up view of the previous photograph. Note the limb-perpendicular fan-patterned foliations and second-order folds along the limb of the larger anticline visible in the previous photograph. Note also the downward grown crystals of some veins.

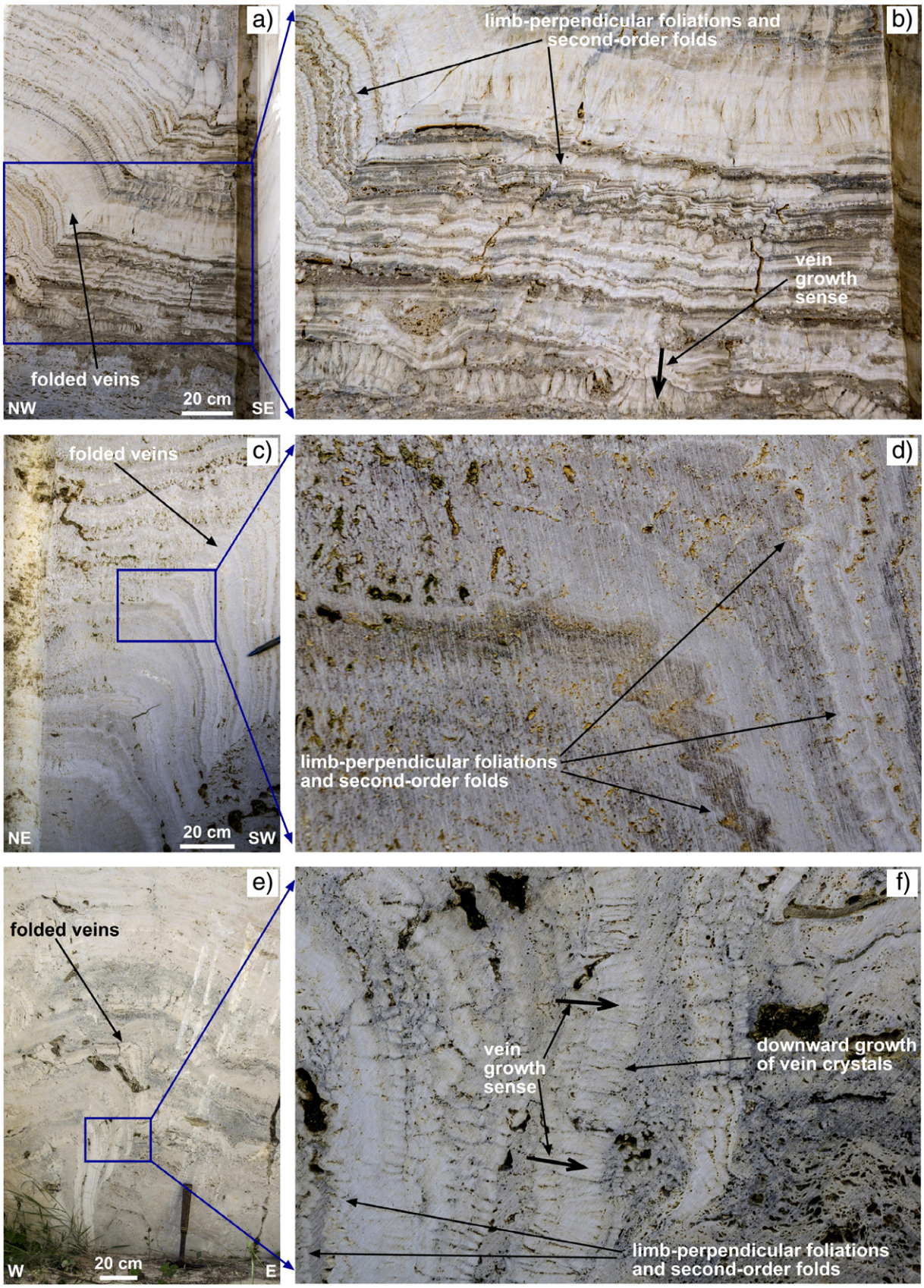
a)
folded veins
NW
20 cm
SE
b)
limb-perpendicular foliations and second-order folds
vein growth sense
c)
folded veins
NE
20 cm
SW
d)
limb-perpendicular foliations and second-order folds
e)
folded veins
W
20 cm
E
f)
vein growth sense
downward growth of vein crystals
limb-perpendicular foliations and second-order folds

structures (Figs. 3a, 4a–c, 5a–b, S4, S11, S12, S15, S16, S22, S37, and S38). In the lower section in contrast, continuously folded veins and beds become dominant and folding progressively more intense. Toward the bottom, the host primary travertine becomes almost completely obliterated by thick veins, and flat beds are almost absent due to the nearly uninterrupted occurrence of folds with various shapes (Figs. 3b, 5f–4h, 6, S7, S9, S13, S14, S17, S18, S21, S25, S26, S28, and S30).

Chimney-like folds correspond to preferential columnar vein growth in short and inclined chevron fold limbs with hinge thickening (Fig. 4a–c). The veins, which are bed-parallel, are often alternated with porous travertine beds in continuity from the short to the long limb of the folds (Figs. S11, S12, S15, S16, S22, and S36–S38). In chimney-like folds, bed-parallel veins are stacked sub-vertically. This stack is often characterized by progressively less steep bed-parallel veins, which thus can form a fan shape in cross-section (Fig. 5a). Vein-parallel stylolites can be observed in most veins, particularly in chimney-like stacks in the short chevron limbs, where stylolites can be seen even macroscopically (Figs. 5a, b, d, S22, and S38).

In many folds, the pristine subcircular pores typical of the bedded porous travertine appear flattened, squeezed, dragged, or totally obliterated close to the fold hinges and the veins or folded veins (Figs. 3b, 5c, d, S6, S11, S12, S14, S23, and S35). Many folds are also characterized by hinge thickening compared with the limbs (Figs. 5f, 6c, d, S9, S15, S25, S27, S29, and S30). When adjacent arrays of flat and undulated beds occur, non-karstic voids can be seen at the contact between them, specifically at the cores of folds, thus forming detachment levels between the flat and folded beds and veins (Figs. 5c, e, S6, and S32). The folded veins and travertine beds are often characterized by folds with different wavelength nested inside each other. Typically, the limbs of large folds contain veins affected by smaller second-order folds with axial surfaces perpendicular to their limbs, thus forming axial-planar foliations. The foliation fans across the folded layers so that it tends to remain perpendicular to the fold limbs (Figs. 5f–g, 6, S9, S13, and S30). Some folds with inclined or even overturned sub-horizontal limbs are characterized by smaller sub-vertical folds affecting the sub-horizontal limbs giving rise to interference patterns typical of refolded folds (Figs. 5h–i, S10, S15, S21, and S26). When observed on sub-horizontal natural pavements, many folds are sub-circular, suggesting 3D domal shapes (Figs. 5j and S39).

3.2. U-Th geochronology

To understand the temporal relationship between veins, folds, and host travertine, we obtained 11 U-Th dates (see the Supplementary material for the methods) that are synthesized in the stratigraphic column of Fig. 7 and reported in Table S1. We mainly dated veins (8 out of 11 samples) as they usually provide more accurate and reliable results than bedded travertines (Uysal et al., 2007, 2009; De Filippis et al., 2012). We also obtained reliable results from two carefully selected samples of bedded travertine (ST4 and CP14_25). Results (Fig. 7b) show a decrease in age toward the top from ~368 to ~107 ka BP (CP14_5 and ST4 samples, respectively). The oldest sample (CP14_5 = 368 ± 14 ka) is a vein, indicating that the host bedded travertine at the same stratigraphic level is older than 368 ± 14 ka. A speleothem sampled within an intra-travertine karst cavity (Fig. 7b) and dated at ~15 ka (ST1_sp1) indicates that the travertine deposit was undergoing weathering at that time. The main result from our radiometric analyses is that four veins are inconsistent with the law of stratigraphic superposition, namely ST3, ST1, CP14_2, and CP15_8. Each of these samples are younger than at least one overlying sample (either vein or host travertine) as shown in Fig. 7(b).

3.3. Stable isotopes

To investigate their origin, understand the differences between primary travertines and hosted veins, and calculate their temperature of formation, we analyzed $\delta^{13}C$ and $\delta^{18}O$ of 61 samples from the Pianetti and of 18 samples from the Pian di Palma quarry (see Supplementary Material for the method). Results are shown in Figs. 8, S40, and S41, and in Table S2. Samples are from the veins or folded veins and related host bedded travertines from five structures in the Pianetti quarry (Fig. S40) and two in the Pian di Palma quarry (Fig. S41).

$\delta^{13}C$ values are positive for all samples, spanning between 5.0 and 6.5‰ (VPDB) for the samples from the Pianetti quarry and between 5.8 and 7.4‰ (VPDB) for the samples from the Pian di Palma quarry. $\delta^{18}O$ values span between −8.9 and −6.1‰ (VPDB) for the samples from the Pianetti quarry and between −6.0 and −5.1‰ (VPDB) for the samples from the Pian di Palma quarry (Fig. 8a and b). The temperature of parental fluids (for both veins and host travertines; Fig. 8c, d, S40, and S41, and Table S2) is addressed and discussed below in the following discussion section.

4. Discussion

4.1. Structures and temporal relationships

The first question arising is whether the observed veins and travertine undulations (folds in Figs. 2–6, and S1–S39) are coeval with or younger than the porous bedded travertine, which we consider the primary deposit. Our field observations and U-Th data show that most veins and undulations are younger than the porous bedded travertine and hence are post-depositional structures. In particular:

(1) In the Pianetti travertine, based on U-Th ages, some folded veins are younger than stratigraphically overlying veins or bedded travertines, showing that multiple rejuvenation processes occurred within this deposit during the Pleistocene (Fig. 7b and Table S1).
(2) At both localities, some veins are characterized by downward radiating crystals (Figs. 4d, e, 6f, S7, S8, S14, S18, S19, and S25), showing that these veins are secondary (late) structures within the host travertine, as they nucleated from an overlying bed and grew downward.
(3) At both localities, many original sedimentary structures such as flat beds and sub-circular pores are dragged, flattened, obliterated or overprinted by veining and folding (Figs. 3b, 5c, d, S6, S11, S12, S14, S23, and S35), demonstrating their post depositional origin. This is also supported by relicts of porous travertine occurring between radiating crystals of veins (Figs. 4c, d, f, g, 5j, S11, S12, S15, S34–S39).
(4) Particularly at Pianetti but also at Pian di Palma, bed- or vein-normal foliations and second-order folds occur nested within the limbs and hinges of larger folds, showing layer-parallel shortening (LPS) during the pre- or early-stages of folding (Figs. 5f–g, 6, S9, S13, and S30).
(5) At both localities, vein-parallel stylolites are well-developed in sub-vertical chimney-like stack of veins (Fig. 5a, b, d, S22, and S38), showing vein-normal compression and carbonate dissolution. More generally, compressional strain markers such as stylolites (Fig. 5a, b, d, S22, and S38), secondary folds with axial plane foliation (Figs. 5f–g, 6, S9, S13, and S30), and pore deformation (Figs. 3b, 5c, d, S6, S11, S12, S14, S23, and S35) indicate post-deposition compression in all directions near the folded veins, possibly with a maximum value in the horizontal direction (LPS).
(6) At Pianetti, some inclined or even overturned large folds are characterized by upright second-order (parasitic) folds, which affect the sub-horizontal limbs of the larger inclined folds. This evidence shows the occurrence of incremental superposed (polyphase) folding induced by sub-horizontal (LPS) contraction (Figs. 5h–i, S10, S15, S21, and S26).
(7) At both localities, post-depositional non-karstic voids occur between folded and flat veins or bedded travertines (Fig. 5c, e, S6,

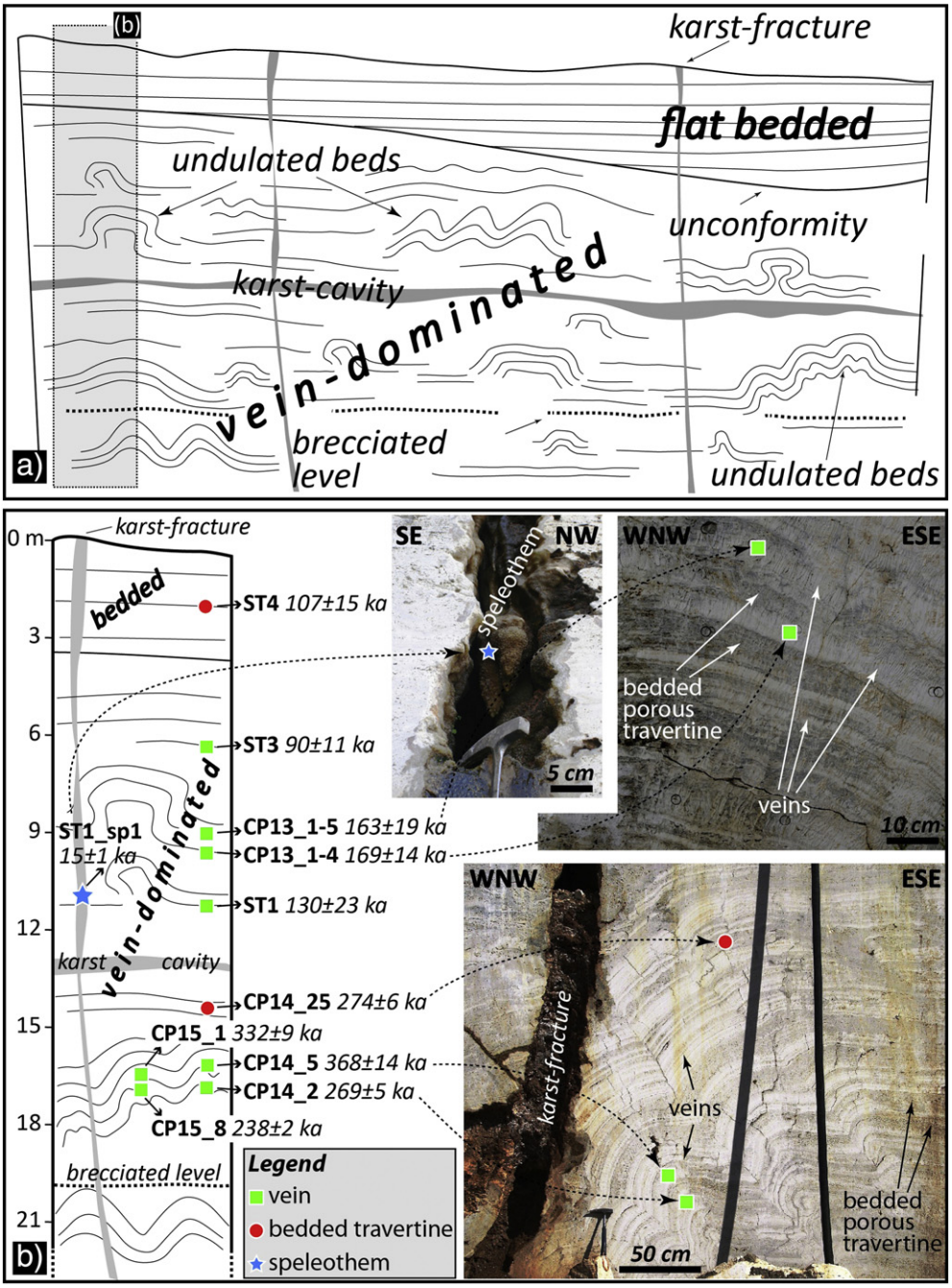

Fig. 7. Synthesis and stratigraphy of radiometric dating results (U-Th) for the Pianetti travertine samples. Complete results are reported in Table S1. (a) Conceptual stratigraphic sketch of the Pianetti deposit. (b) Stratigraphic log/sketch (left) from the Pianetti deposit with sample location (depth) and age. Note that four veins are inconsistent with the law of stratigraphic superposition, namely ST3, ST1, CP14_2, and CP15_8. Each of these samples are indeed younger than at least one overlying sample (either vein or host travertine). Photographs (right) show some of the sample location.

and S32). Voids, in particular, are located in the core of folds, indicating that the folds (or undulation) cannot be *syn*-depositional; otherwise the voids would have been immediately mineralized and filled by the same fluids that generated the primary travertine beds.

4.2. Parental fluid temperatures

The temperature of carbonate precipitation can be estimated using the oxygen isotope thermometer (McCrea, 1950). This thermometer is based on the temperature dependence of the calcite-water oxygen isotope fractionation and requires the knowledge of the $\delta^{18}O$ of the carbonates and the precipitating water. The oxygen isotope composition of the mineralizing parental fluids can only be estimated introducing uncertainty in the calculated temperatures. Furthermore, this method assumes equilibrium fractionation during travertine formation, which is not necessarily true in all travertine depositional environments (Kele et al., 2008, 2011, 2015; see also Beaudoin et al., 2014, for other types of $CaCO_3$ precipitates). Here we calculate the temperatures of precipitation using the calibration of Kele et al. (2015), which is based on recent travertines. We note that this equation is based on samples collected close to the vents, carbonate scalings inside tubes of thermal wells, and carbonates precipitated in pools, which are the only travertines representing "close-to-equilibrium" precipitation (Kele et al., 2015). In our study cases, the temperatures are calculated using a fluid

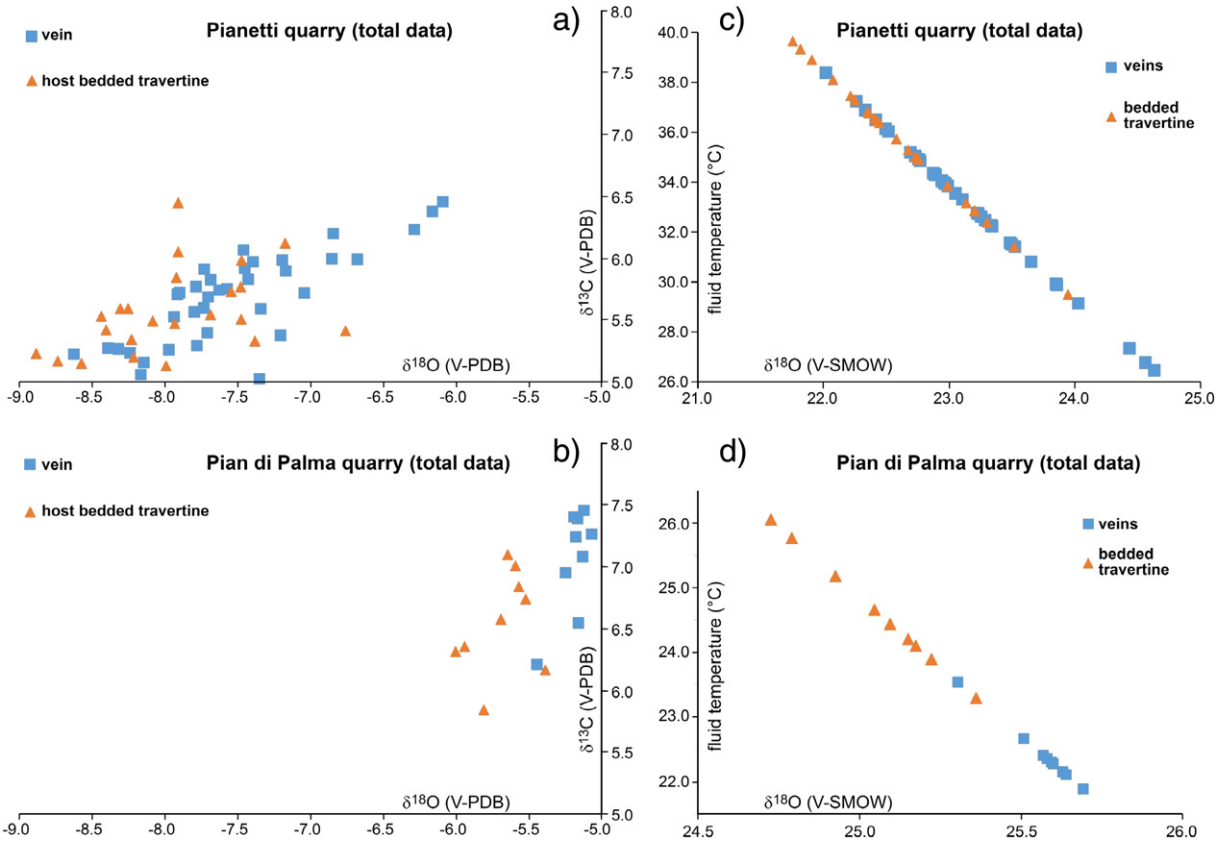

Fig. 8. Stable isotope data. Complete results are reported in Table S2 and further shown in Figs. S40 and S41. (Left) C- vs. O-isotope ($\delta^{13}C$ vs. $\delta^{18}O$) diagrams for samples from the (a) Pianetti and (b) Pian di Palma quarries. Note that the Pianetti and Pian di Palma travertines are thermogene as they fall within the typical $\delta^{13}C$ interval of thermogene travertines (between −1 and +10‰ PDB; Pentecost, 2005). (Right) Parental fluid temperature vs. O-isotope ($\delta^{18}O$) diagrams for samples from the (c) Pianetti and (d) Pian di Palma quarries.

$\delta^{18}O$ of −6.4‰ VSMOW, which is the present $\delta^{18}O$ value from the Saturnia Spring hydrothermal waters, where thermogene travertines are being actively precipitated in a locality that is between the Pianetti (1.7 km distant) and Pian di Palma (5 km distant) quarries (Fig. 1c).

The differences in $\delta^{18}O$ between bedded travertines and vein calcites (Figs. 8c, d, S40, and S41, and Table S2) can be interpreted as due to the: (1) difference in the temperature of parental fluids; (2) kinetic effects during carbonate deposition; and (3) difference in the $\delta^{18}O$ of the parental fluids.

(1) In the $\delta^{13}C$ vs. $\delta^{18}O$ diagrams (Fig. 8a and b), we observe that the bedded travertines are generally characterized by $\delta^{18}O$ values slightly more negative than the veins. This pattern could be explained with parental fluid temperatures on average 1–3 °C warmer for the bedded travertine than for the veins (Fig. 8c and d, Table S2).
(2) In an open-air environment (bedded porous travertine), the fast pressure drop and CO_2 volatilization causes immediate $CaCO_3$ precipitation at the spring temperature. In contrast, in an intralithic environment (veins), CO_2 degassing and consequently $CaCO_3$ precipitations are slower possibly with a slight cooling of the fluids.
(3) An alternative explanation for the different $\delta^{18}O$ values of the bedded travertines and veins could be a difference in the $\delta^{18}O$ values of their parental fluids.

Based on the above considerations, we interpret the difference in the calculated temperatures of parental fluids mainly related to the difference in the precipitation kinetics accompanied by a slight cooling of precipitating fluids in the veins, thus corroborating our field observations showing the occurrence of post-depositional veins. Our temperature data remain to be confirmed in the future by, for instance, clumped isotopes (Ghosh et al., 2006; Eiler, 2007; Kele et al., 2015).

4.3. Vein and fold development

We interpret the veins and folds as post-depositional structures developed within and/or at the expense of the primary porous bedded travertine. Radiometric dating shows that, during Pleistocene time, vein emplacement occurred progressively from bottom to top in the bedded travertines while the primary travertine beds were still forming in the upper portion of the deposit (Figs. 7 and 9). Veins, in particular, are characterized by subhedral crystals with growth competition textures (e.g., Fig. 4c–e) indicating that the crystals slowly precipitated in fluid-filled pores with continuous advection of a supersaturated solution (Hilgers et al., 2004). Isotope data confirm that the mineralizing thermogene fluids at the origin of veins and bedded travertine are very similar (Fig. 8). $\delta^{13}C$ values are all consistent with a thermogene origin for both travertines and veins (i.e., between −1 and +10‰ PDB; Pentecost, 2005). The C- and O-isotope range is typical of Pleistocene-Holocene thermogene travertines in Tuscany and central Italy (Fig. 8; Manfra et al., 1976; Gandin and Capezzuoli, 2008; Berardi et al., 2016; Vignaroli et al., 2016 and references therein). The radiometric data (~368–90 ka; Fig. 7b) indicate a close temporal association of both travertine deposition at the surface and vein precipitation at depth with the (paroxysmal) volcanic activity from the adjacent Amiata and Vulsini districts (between about 600 and 100 ka BP; Nappi et al., 1995; Cadoux and Pinti, 2009; Laurenzi et al., 2015).

Collectively, the field, geochronological, and isotope evidence indicates that the freshly deposited bedded travertines were soon diagenetically-altered through incremental veining from the same hydrothermal

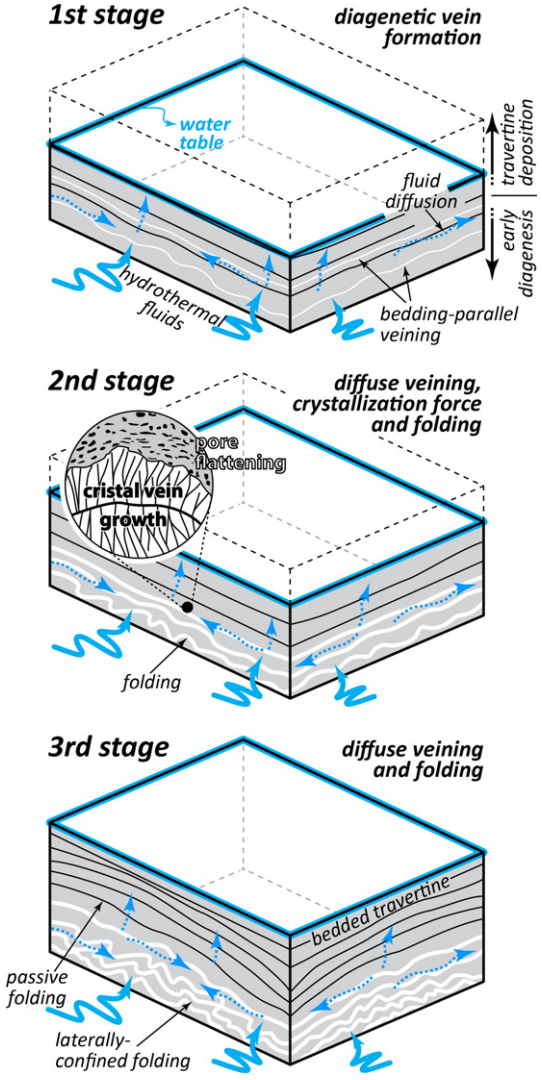

Fig. 9. General conceptual model of travertine deposition and post-depositional progressive formation of non-tectonic bed-parallel veins and folds. Domal folds are driven by laterally-confined *syn*-diagenetic mineralization (volume expansion generating horizontal layer parallel shortening, LPS) induced by a continued hydrothermal supply coming out from under the travertine.

fluids that had generated (at the deposit bottom) and were still generating (at the deposit top) the primary porous travertine beds (Fig. 9). We interpret the studied travertine and vein folding as the product of post-depositional *syn*-diagenetic deformation. The deformation is not of tectonic origin both for their domal shape (Fig. 5j) and for the substantial absence of other compressional structures in the host sediments of the Albegna basin (Brogi, 2008; Carmignani et al., 2013; Berardi et al., 2016; Vignaroli et al., 2016). The travertine folds must have therefore originated through *syn*-diagenetic progressive and incremental vein growth (Fig. 9). In general, we believe that, in a laterally-confined environment offered by the host sediments and primary bedded travertines themselves, the *syn*-diagenetic volume expansion caused by the vein growth resulted into a regime of horizontal LPS, which caused the progressive folding of the vein-host assembly and the consequent vertical layer-normal expansion as shown in Fig. 9. Horizontal veining and fold amplification with vertical veins in fold limbs were likely driven by the crystallization force (Taber, 1916; Weyl, 1959; Assereto and Kendall, 1977; Watts, 1978; Fletcher and Merino, 2001; Wiltschko and Morse, 2001; Hilgers and Urai, 2005; Noiriel et al., 2010; Gratier et al., 2012) associated with vein development and continuous fluid supply. In this process, the fan-like radiating growth of vein crystals (Figs. 4c–f, 5c, and 5d, S6–S8, S11, S14, S18, S19, S25, S31, S34, S35, and S37) must have had a determinant role, exerting a crystallization force with both vertical (i.e., vein-normal) and horizontal (i.e., vein-parallel) components.

The geometrical complexity of many observed folds (Figs. 3–6 and S1–S39) implies complex folding mechanisms associated to post-depositional incremental veining. We attempt to model and explain in detail the travertine folding as inferred from the structure observations, with the knowledge that the ones proposed are only geometric and kinematic possible models and that the observed finite strain, in many cases, is possibly the result of a spatio-temporal complex combination of multiple deformation mechanisms.

We start assuming that vein development is driven by the crystallization force. This means that a flux of CO_2-rich fluid saturated in carbonate comes from depth (Fig. 9). At large depths, fluids are in equilibrium with carbonates, whereas, when rising up, the fluids are characterized by a progressive pressure decrease. Consequently, at some critical depth, the CO_2 degassing leads to a drastic supersaturation of the fluid and carbonate precipitation. The force of crystallization is proportional to the surpersaturation and may be largely higher than the weight of the rocks above the horizontal (bed-parallel) veins, consequently leading to the uplift of the overlying travertine pile (a1 in Fig. 10a; Gratier et al., 2012).

If the vein growth occurs within the travertine pile, at a depth above the base of the pile, the shape of the surface of the travertine pile may influence the shape of the veins that appear to be bent (a′2 in Fig. 10a). A free lateral surface on the flanks of the travertine pile may even favor the development of asymmetric folds, a very common feature in gravity sliding processes, which would be associated here with the deformation of the travertine flanks (a′n in Fig. 10a).

Alternatively, if the development of the veins occurs in the basal section of the travertine pile (Fig. 9), hence in confined conditions (Fig. 10b; i.e., we believe that this is the case for most of our observed folds as illustrated in Fig. 9), the development of the veins will induce internal stress with the maximum compressive components (the arrows in Fig. 10b) that are perpendicular to the vein surface. To fold the initially horizontal travertine porous beds or the secondary horizontal veins, there are at least two possibilities:

(1) The first possibility is the development of vertical veins (b2 in Fig. 10b). The opening of a vein by crystallization force, independently of its orientation, must oppose at least three types of forces: (i) the tensional strength of the rocks to initiate the fracture opening, (ii) the component of stress perpendicular to the vein surface, and (iii) the strength linked to a possible collapse of the porosity of the rocks (as the process occurs within highly porous rocks). The sum of these three components gives the minimum energy required to open a vein by crystallization force. If the opening of a vertical vein is less energy-consuming than the opening of a horizontal vein, then a vertical vein will develop. In non-tectonic environments, it is likely that, due to the anisotropic bedded structure of travertines, the vertical tensional strength of the rocks is lower than the horizontal one, thus favoring the development of horizontal veins provided that the two other strength components (stress and compressibility) are the same; however, a very small difference may lead to vertical vein formation. Due to the absence of vertical (across beds) veins in the studied exposures, we believe that this (b2 in Fig. 10b) should not be the appropriate mechanism for most of the Pianetti and Pian di Palma folds. It remains, however, a suitable mechanism in similar diagenetic environments (see next section; e.g., Handford et al., 1984).

(2) Alternatively, if the development of horizontal veins is not homogeneous in thickness, local overdevelopment may lead to fold initiation and then progression toward either chevron folds (b′2 to b′n in Fig. 10b) or buckle folds (b″2 to b″n in Fig.

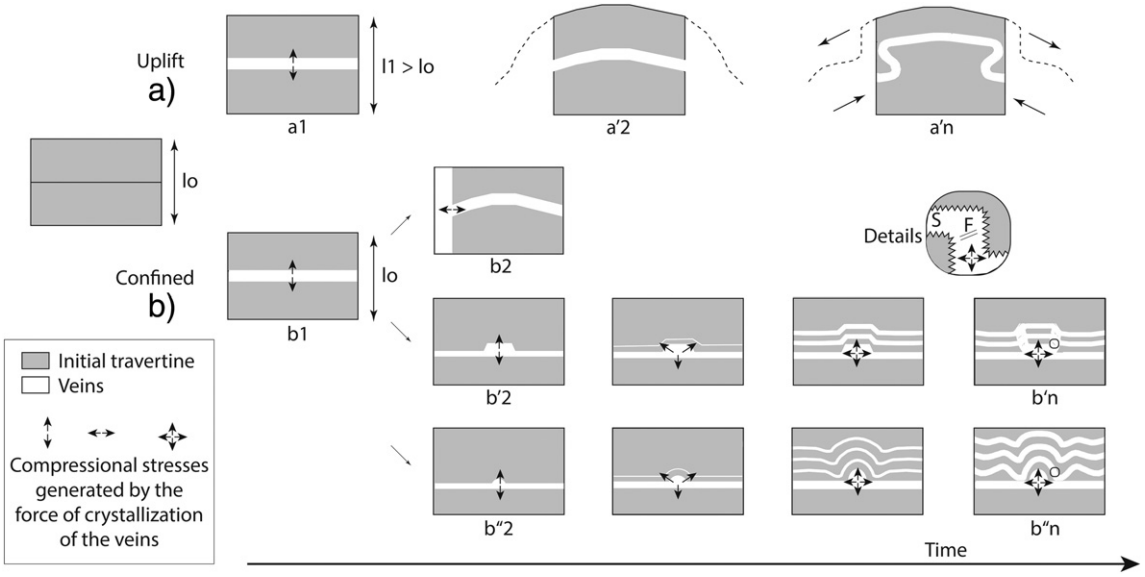

Fig. 10. Conceptual model of vein growth under the effect of crystallization force that may lead to various folded structures. (a) within the travertine pile, veins may grow parallel to the upper surface, uplift this upper part and evolve to asymmetric folds with gravity sliding (a′1 to a′n). (b) Within the lower level of the travertine pile surface, in a confining space, the development of vertical vein may lead to the folding of the horizontal veins and travertine beds (b2). Alternatively, irregular growth of the horizontal veins may lead to chevron folds (b′2 to b′n) or buckle folds (b″2 to b″n) initiation and development. Inset shows the details of microstructures: stylolite parallel to the veins (S) and foliation (F). The arrows indicate compressional stress induced by crystallization force during vein growth.

10b). As discussed above, the development of the vertical limbs of the folds will be easier if the energy needed to open vertical or horizontal veins is not very different. The development of compressive stresses, which are induced in all directions by the vein growth, will tend to develop compressive structures in all directions as we observed in our outcrops. Relevant examples are the secondary folds within the folded veins (Figs. 5f–g, 6, S9, S13, and S30), pore flattening (Figs. 3b, 5c, d, S6, S11, S12, S14, S23, and S35), or stylolites at the boundary of the veins (Figs. 5a, b, d, S22, and S38). It is difficult to evaluate the accurate compressive strain values in all directions. In our model (Fig. 10), for simplicity, we assume that the opening of the veins by crystallization force is compensated by compressive strain around them. We believe that these mechanisms (confined; b′n and b″n in Fig. 10b) are the most suitable ones to explain most observed folds (Figs. 3–6, and S1–S39). In particular, the columnar stacking of bed-parallel veins and the radiating growth of vein crystals must have had an important role, respectively, in initiating chevron (or chimney-like) folds (e.g., Fig. 5a) through a mechanism of bending and in driving buckle-folds (e.g., Fig. 5c) through a mechanism of LPS (b′n and b″n in Fig. 10b).

As explained above, fold hinge thickening and the occurrence of second-order folds and fan-patterned foliations nested within the folds (e.g., Figs. 5f, g, and 6) suggest that part of them must have developed through buckling. Assuming a Newtonian viscosity, the Biot-Ramberg's buckling equation states that the arc length-thickness (L/t) relationship for a thin folded bed with viscosity η_B surrounded by a matrix with viscosity η_M is:

$$L/t = 2\pi(\eta_B/6\eta_M)^{1/3} \quad (1)$$

Measuring L and t of the veins folded to form the second-order small folds observed in Figs. 5(f), 5(g), and 6 (Table S3), we estimate η_B/η_M being between 1.5 and 4. In other words, the host bedded travertine was non- or poorly-consolidated and therefore 1.5–4 times less viscous than the veins at the time of buckle-fold formation. Although this estimate provides only an approximate value for the rheological contrast between single veins and host bedded travertine at the time of folding, it supports the hypothesis of a *syn*-diagenetic origin of veins and folds and therefore of a viscosity increase induced by diagenesis. Therefore, we hypothesize that also the data by Ronchi and Cruciani (2015), who measured bulk porosities between less than 3% and ~35% in the Pianetti and Pian di Palma travertines, may be interpreted as due to a significant reduction of porosity (from 35 to 3%) induced by pore collapse and cementation during *syn*-diagenetic veining and folding.

4.4. Analogies, general applicability, and disputes

4.4.1. Similar structures elsewhere

Analogously to the Pianetti and Pian di Palma deposits, primary porous beds and secondary veins have been frequently recognized in thermogene travertines elsewhere (Uysal et al., 2007, 2009; De Filippis and Billi, 2012; De Filippis et al., 2012, 2013a, 2013b; Gratier et al., 2012; Frery et al., 2015, 2016; Berardi et al., 2016; Ünal-İmer et al., 2016; Vignaroli et al., 2016). In particular, thick-banded veins often

Fig. 11. Examples from other thermogene travertine deposits. (a) Veins within Pamukkale travertines (Denizli, Turkey; Uysal et al., 2009). Note the vertical "intrusion" (similar to a dike) of the banded vein through horizontal travertine beds and a set of departing sill-like banded veins along the travertine beds. (b) Antiformal vein across and along the bedded porous travertines forming the Kamara fissure ridge (Denizli, Turkey; De Filippis et al., 2012). (c) Antiformal vein across and along the bedded porous travertines forming the Kocabaş fissure ridge (Denizli, Turkey; De Filippis et al., 2012). (d) Veins within the Colle Fiorito fissure ridge (Tivoli, Italy; De Filippis et al., 2013a). Note the vertical "intrusion" (similar to a dike) of the banded vein through horizontal travertine beds and the departing sill-like banded vein along the travertine beds. (e) Veins (post-depositional as demonstrated by dating and microscopic evidence of downward growth) within Crystal Geiser (Utah, USA) travertine beds (Gratier et al., 2012). The antiformal white veins, in particular, form sill-like structures along pre-existing travertine beds. (f) Specimen of travertine veins from Denizli (Turkey; Özkul et al., 2013). Note the presence of a complex array of banded veins, which are undulated at the centimetric scale similarly to many veins observed in the Pianetti and Pian di Palma travertines (Fig. 6). (g) and (h) Folded bed-parallel veins alternated with porous bedded travertine from Tivoli (central Italy). Note the similarity between these structures and those from the Pianetti and Pian di Palma travertines shown in Figs. 3–6. (i) Alternations of inclined porous bedded travertine and veins from Acquasanta (central Italy). Below, in the two insets, note that the veins are characterized by opposite patterns of radiating crystals indicating opposite senses of growth, i.e., upward (left inset) and downward (right inset). At least the vein (the upper one) with the downward sense of growth has to be post-depositional.

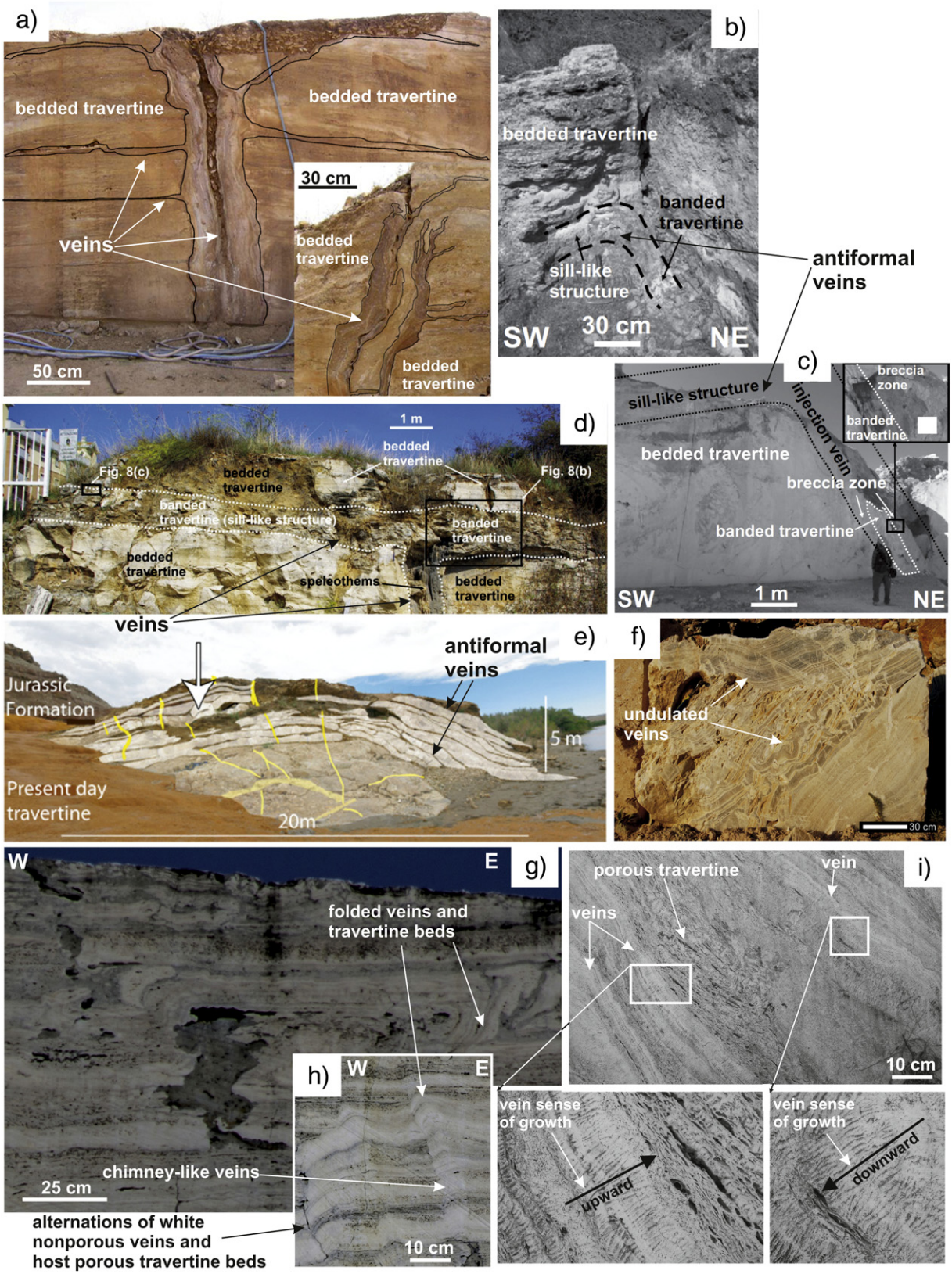
a)
bedded travertine
bedded travertine
veins
30 cm
bedded travertine
bedded travertine
50 cm
b)
bedded travertine
banded travertine
sill-like structure
antiformal veins
SW
30 cm
NE
c)
sill-like structure
injection vein
breccia zone
banded travertine
bedded travertine
breccia zone
banded travertine
SW
1 m
NE
d)
1 m
bedded travertine
Fig. 8(c)
bedded travertine
Fig. 8(b)
banded travertine (sill-like structure)
banded travertine
bedded travertine
speleothems
bedded travertine
veins
e)
antiformal veins
Jurassic Formation
5 m
Present day travertine
20m
f)
undulated veins
30 cm
W
E
g)
folded veins and travertine beds
chimney-like veins
25 cm
alternations of white nonporous veins and host porous travertine beds
h)
W
E
10 cm
i)
porous travertine
vein
veins
10 cm
vein sense of growth
upward
vein sense of growth
downward

cut through the axial portion of fissure ridge travertines. From these axial veins, lateral ramifications can depart and develop along the host beds in a sill-like fashion, lifting the overlying travertine beds and forming, in some instances, gently arched (antiformal) structures (Fig. 11a–e; Uysal et al., 2009; De Filippis et al., 2012, 2013a; Gratier et al., 2012). Structures of this type are observed in thermogene travertines from Denizli (Turkey), Tivoli (Italy), Crystal Geyser (Utah), Bridgeport (California), and elsewhere (De Filippis et al., 2012 and references therein). These veins have been radiometrically dated or interpreted on the basis of crosscutting relationships as due to post-depositional processes. They occur in shallow environments, a few meters to a few tens of meters depth, possibly in relation to seismic events (Uysal et al., 2007, 2009), with the vein horizontally dilating or vertically uplifting the host beds thanks to the crystallization force (De Filippis et al., 2012; Gratier et al., 2012).

In the Tivoli and Acquasanta quarries (central Italy), undulated bed-parallel veins hosted within the late Pleistocene travertine beds can be observed. These veins are shown in Figs. 11(g)–(h) and are very similar to those observed at Pianetti and Pian di Palma (Figs. 3–6 and S1–S39). In particular, a series of inclined porous beds alternating with bed-parallel veins were observed at Acquasanta. The veins show upward and downward radiating patterns of growth (Fig. 11i) explainable only with a post-depositional bed-parallel mineralization and downward growth of vein crystals (at least for the upper veins that grew downward; see close-up photograph in the lower right inset of Fig. 11i). These examples from Italy, Turkey, and USA (Fig. 11) suggest that secondary veins and folds as well as rejuvenation processes similar to those observed and inferred at the Pianetti and Pian di Palma quarries may be a common feature of thermogene travertines (e.g., Uysal et al., 2007, 2009; De Filippis and Billi, 2012; De Filippis et al., 2012, 2013a, 2013b; Gratier et al., 2012; Frery et al., 2015, 2016; Berardi et al., 2016; Ünal-İmer et al., 2016; Vignaroli et al., 2016). In particular, veining able to uplift the rock above the vein with the force of crystallization is probably the most common process (Fig. 11; Gratier et al., 2012; De Filippis et al., 2013a). We believe that diagenesis and possible rejuvenation of thermogene travertines are open and challenging tasks for future studies.

In relation to the Tivoli deposit in central Italy, it is interesting that this thermogene travertine is characterized by an uppermost zone of a very porous flat bedded travertine named Testina (Faccenna et al., 2008; De Filippis et al., 2013a, 2013b). The Testina is a few meters thick and contrasts with the very compact, far less porous, and up to 80 m thick underlying travertine. Manfra et al. (1976), based on chemical and isotopic analyses, concluded that the Testina layers may represent a pristine poorly- to non-cemented travertine in contrast with the underlying compact diagenetically-cemented and -altered deposit. This setting (i.e., vertical zonation) is similar to those of the Pianetti and Pian di Palma quarries, where bed-parallel veins occur in the lower and intermediate portions of the travertine deposits and are substantially absent or poorly frequent in the upper portions (Figs. 2 and 7a).

4.4.2. Different interpretations

Structures very similar to those observed in this study and interpreted as post-depositional folds were previously reported from other thermogene travertine deposits and interpreted as primary depositional features. We refer, for instance, to antiformal structures interpreted as pool rims or lips in the travertine deposits of Rapolano Terme (Italy; Fig. 12a–d), Mammoth Hot Springs (USA; Fig. 12f), and elsewhere (e.g., Hammer et al., 2007). It is not our intention here to re-interpret these structures. We only observe that, at least in the structures shown in Fig. 12(c) and (f), the upright limb of the pool rims is characterized by bed-normal foliations and small folds (similarly to travertine folds in Fig. 6), whose interpretation as primary depositional features is, in our opinion, problematic. These structures could indeed be interpreted as due to LPS as in Figs. 5(f), (g), and 6.

Based on our observations, we suggest that the origin of some structures in thermogene travertines may need to be reevaluated and that further research on this subject is necessary. To contribute to this discussion, we propose a list of significant criteria to discriminate secondary from primary structures and to identify rejuvenation processes:

(1) Radiometrically-dated structures younger than overlying ones (e.g., Fig. 7b);
(2) Downward growth of crystals (e.g., Fig. 4d);
(3) Veins overprinting/cutting through overlying or underlying beds (e.g., Figs. 3a and 4f);
(4) Relicts of primary porous travertine beds between vein radiating crystals (e.g., Fig. 4g);
(5) Deformed primary structures such as beds or pores in approaching veins and folds (e.g., Figs. 3b and 5c);
(6) Bed-normal foliations and second-order folds (consistent with LPS) nested inside larger folds (e.g., Fig. 6);
(7) Polyphase folding including overturned folds with refolded limbs (e.g., Fig. 5i);
(8) Stylolite surfaces parallel and stylolite teeth normal to vein planes (e.g., Fig. 5a);
(9) Post-depositional non-karstic voids between folded and flat veins and beds, outlining the occurrence of post-depositional detachment mechanisms between adjacent beds (e.g., Fig. 5e).

We believe that the occurrence of one or more of the above-mentioned evidence if it is not really conclusive is at least strongly suggestive of travertine post-depositional *syn*-diagenetic processes such as veining, folding, or rejuvenation actions.

4.4.3. Analogous and inverse structures in different environments

We also evaluate whether the proposed mechanism of veining and folding (Figs. 9 and 10) is unique for travertines or otherwise is applicable to other diagenetic environments. In many evaporites, undulated veins similar to those observed in thermogene travertines are common in layers or veins of gypsum, anhydrite, halite, and carbonate (Fig. 13a and b). These undulations are known as post-depositional folds developed owing to a mineral-growth-related volume expansion in shallow but laterally-constrained environments so that the originally-flat evaporitic layers become contorted through LPS and consequent buckling (West, 1965; Hussain and Warren, 1989; Tompkins et al., 1994; Aref et al., 1997; Sumner, 1997; Gandin et al., 2005; Gündogan et al., 2005; Schreiber and Helman, 2005). These folded veins or layers are commonly named enterolithic for their resemblance with intestines (Fig. 13b). As stated by Gandin et al. (2005), enterolithic folds are "the result of vertical expansion during rehydration, showing typical subvertical, isoclinal folds and wavy, overturned, crest lines. Folding may be more open, and often develops into small thrusts." This statement is also mostly applicable (except for the rehydration process that is typical of evaporitic anhydrite), in our opinion, to many folds studied in this paper (e.g., Figs. 2d and S5).

The same deformation mechanism or a very similar one is also proposed for the development of non-tectonic *syn*-diagenetic folds and antiformal tepee structures in intertidal-peritidal vadose carbonate rocks. In such an environment, carbonate precipitation in fractures and pores from peritidal brines and meteoric waters can generate volume expansion in laterally-confined shallow beds (i.e., displacive carbonate cement according to Watts, 1978) that consequently buckle, forming antiformal tepee structures (Fig. 13c; e.g., Assereto and Kendall, 1977; Handford et al., 1984; Kendall and Warren, 1987; Enos et al., 2006; Lokier and Steuber, 2009). The above-mentioned tepee structures and enterolithic folds (Fig. 13) substantiate the *syn*-diagenetic deformation and rejuvenation model proposed for the travertine veins and folds studied in this paper (Figs. 9 and 10).

To corroborate our hypothesis of *syn*-diagenitic contractional deformation for the Pianetti and Pian di Palma thermogene travertines, we also propose an inverse *syn*-diagenetic analogy. In our hypothesis, the

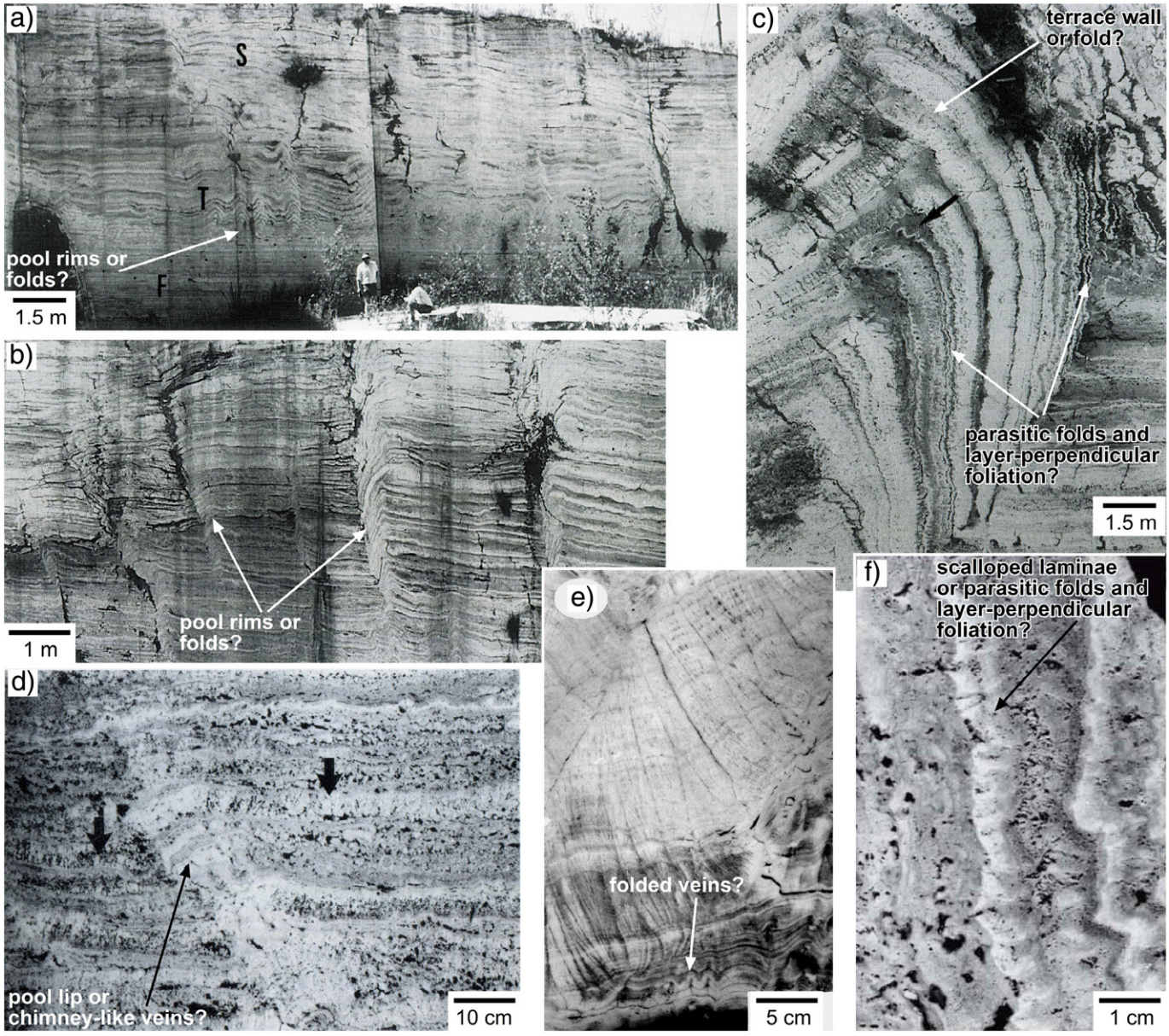

Fig. 12. Travertine undulated structures similar to those shown in this paper in Figs. 3–6 and S1–S39 are interpreted as primary depositional structures and not as secondary *syn*-diagenetic veins and folds. In this figure, some examples from the previous literature are shown. In the photographs, possible contrasting interpretations are reported with question marks. (a), (b), and (c) Travertines from Rapolano Terme, central Italy (Guo and Riding, 1994, 1998). (d) Travertines from Rapolano Terme, central Italy (Chafetz and Folk, 1984). (e) Travertines from Bagni di Tivoli, central Italy (Chafetz and Guidry, 1999). (f) Travertines from Mammoth Hot Springs, Yellowstone National Park, Wyoming (Chafetz and Guidry, 2003).

observed travertine folds indeed formed mostly by *syn*-diagenetic LPS resulting from volume expansion (veining) in a laterally confined environment (Figs. 9 and 10). In other diagenetic settings (i.e., marine basins), the inverse mechanism can also be true. We refer, in particular, to polygonal normal faults that are non-systematically-oriented, intraformational, *syn*-diagenetic (very rarely tectonic; e.g., Petracchini et al., 2015), normal faults affecting many marine sedimentary basins. Polygonal normal faults develop as non-tectonic structures during diagenesis in response to laterally-heterogeneous volume changes (i.e., heterogeneous vertical thinning) caused by or associated to laterally-heterogeneous mechanisms and parameters such as sediment compaction, fluid flow and pressure, gravitational loading, and chemically driven volumetric contraction or syneresis (Cartwright and Lonergan, 1996; Cartwright and Dewhurst, 1998; Cartwright, 2011; Antonellini and Mollema, 2015). In our opinion, polygonal normal faults and the travertine folds studied in this paper can be considered as opposite endmembers (i.e., extensional and contractional, respectively) of *syn*-diagenetic deformation in laterally-confined volumes. In other words, it is not surprising that *syn*-diagenetic non-tectonic volume changes of sediments (either expansion or contraction) can generate sediment deformations that are very similar to tectonic deformations such as faults, veins, and folds (e.g., Assereto and Kendall, 1977; Gandin et al., 2005; Cartwright, 2011).

5. Conclusions, limitations, and recommendations for future studies

(1) The studied travertines constitute a hybrid between sedimentary and hydrothermal deposits. A primary travertine host formed (i.e., precipitated) according to the law of stratigraphic superposition. This deposit was next *syn*-diagenetically altered (at least physically if not chemically and mineralogically) from the bottom toward the top by the same hydrothermal fluids from which the host itself precipitated. The resulting rock is characterized by alteration and rejuvenation fronts and structures that are

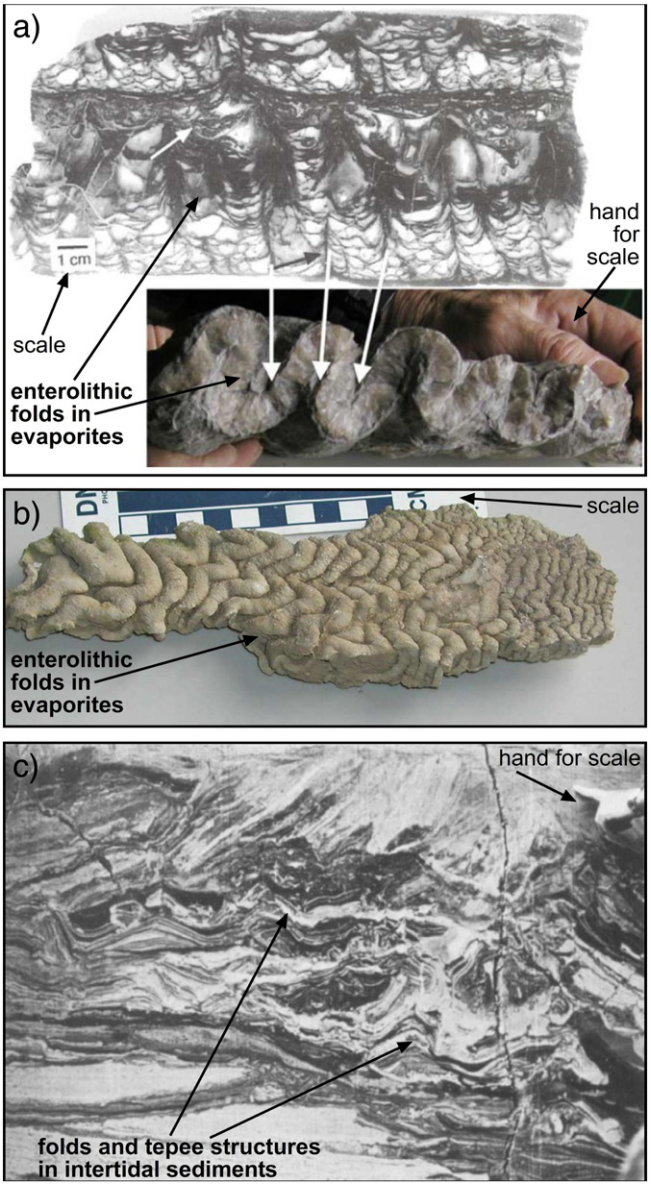

Fig. 13. Non-tectonic *syn*-diagenetic deformations: enterolithic folds in evaporites and folds and tepee structures in peritidal carbonates. (a) Examples of enterolithic folds in evaporites from the Gamohan Formation, South Africa. For further details see Sumner (1997) and Gandin et al. (2005). (b) Example of enterolithic gypsum from evaporites (Gandin et al., 2005). As stated by these authors, this example is "the result of vertical expansion during rehydration, showing typical subvertical, isoclinal folds and wavy, overturned, crest lines. Folding may be more open, and often develops into small thrusts." (c) Example of folds and tepee structures in Triassic peritidal carbonates from Val Brembana, northern Italy. For further details see Kendall and Warren (1987).

increasing downward (i.e., diagenetic/hydrothermal zonation).

(2) The continuous *syn*-diagenetic supply of CO_2-rich fluids can thus diagenetically alter and rejuvenate a primary thermogene travertine modifying some of its original properties including fabric, porosity, chronological sequence, and rheology. It should not be surprising to find veins, alteration fabrics, and other secondary structures in thermogene travertines as it happens in most hydrothermal settings, where hydrothermal fluids keep circulating in the host rock also after its primary formation/precipitation or early alteration, hence adding veins and mineralization to the host, and altering its original fabric and mineralogy.

(3) Among other post-depositional changes, we point out the variation of travertine porosity induced by veining and folding. After the recent discovery of major hydrocarbon reserves in subsalt travertine-like porous rocks along the Atlantic Brazilian and Angolan margins, such porosity variation appears as very relevant for the hydrocarbon industry and worthy of further study.

(4) Similar *syn*-diagenetic structures at various scales in other thermogene travertine deposits and also in different sedimentary environments indicate that those reported in this paper from southern Tuscany may be structures more common than previously thought. This will be an open and challenging task for future studies.

(5) The identification of *syn*-diagenetic structures (e.g., veins and folds) and related changes of rock properties (e.g., age rejuvenation) is relevant for the frequent use of thermogene travertines for the reconstruction of geological processes, paleoclimate oscillations, earthquake occurrences, hydrothermal circulations, and uplift or incision rates. The diagenetic alteration, if unrecognized, may significantly impact or even bias travertine-based 4D geological reconstructions and assessments.

(6) Based on results from this study, we drew a set of nine main geological criteria to discriminate between primary and secondary structures in thermogene travertines. In suggesting the use of these and further criteria in the future when studying and sampling thermogene travertines, we also acknowledge that most structures shown in this paper were interpreted using all or a few of these criteria. A few structures, however, due to outcrop inaccessibility or to lack of evidence, were simply interpreted by analogy and resemblance with the majority of structures for which we had a reasonable number of evidence (criteria) for their interpretation. These limitations together with the different interpretation of similar structures elsewhere (e.g., Fig. 12) impose caution when studying thermogene travertine structures (i.e., are they primary or secondary?) and require future confirmations of our results both in the studied sites and elsewhere in thermogene travertine deposits.

Acknowledgments

Institutional funding from Roma Tre University, CNR-IGAG, Hungarian Academy of Sciences (János Bolyai scholarship to S.K.), Hungarian Scientific Research Fund (OTKA 101664), ETH Zürich, and ISTerre Grenoble are acknowledged. U-Th dating at the HISPEC was supported by the Taiwan ROC MOST grants (105-2119-M-002-001to CCS), and National Taiwan University (105R7625 to CCS). We acknowledge, in particular, no industrial funding for this study. P. Agard, N. Beaudoin, J. Major, and an anonymous reviewer are warmly thanked for the editorial work and constructive comments. Saturnia Travertini Cave srl is thanked for kindly granting our access to the Pianetti di Montemerano quarry.

Appendix A. Supplementary data

Supplementary data associated with this article can be found in the online version, at http://dx.doi.org/10.1016/j.tecto.2017.02.014. These data include the Google map of the most important areas described in this article.

References

Antonellini, M., Mollema, P.N., 2015. Polygonal deformation bands. J. Struct. Geol. 81, 45–58.

Aref, M.A.M., Attia, O.E.A., Wali, A.M.A., 1997. Facies and depositional environment of the Holocene evaporites in the Ras Shukeir area, Gulf of Suez, Egypt. Sediment. Geol. 110, 123–145.

Assereto, R., Kendall, C.G.St.C., 1977. Nature, origin and classification of peritidal tepee structures and related breccias. Sedimentology 24, 153–210.

Barberi, F., Buonasorte, G., Cioni, R., Fiordelisi, A., Foresi, L., Iaccarino, S., Laurenzi, M.A., Sbrana, A., Vernia, L., Villa, I.M., 1994. Plio-Pleistocene geological evolution of the

geothermal area of Tuscany and Latium. Memorie Descrittive della Carta Geologica d'Italia 49, 77–133.
Barberi, F., Innocenti, F., Ricci, C.A., 1971. Il magmatismo dell'Appennino Centro Settentrionale. Rendiconti della Società Italiana di Mineralogia e Petrologia. 27, pp. 169–210.
Batini, F., Brogi, A., Lazzarotto, A., Liotta, D., Pandeli, E., 2003. Geological features of the Larderello-Travale and Monte Amiata geothermal areas (southern Tuscany, Italy). Episodes 26, 239–244.
Beasley, C.J., Fiduk, J.C., Bize, E., Boyd, A., Frydman, M., Zerilli, A., Dribus, J.R., Moreira, J.L.P., Capeliero Pinto, A.C., 2010. Brazil's subsalt play. Oilfield Rev. 22, 28–37.
Beaudoin, N., Bellahsen, N., Lacombe, O., Emmanuel, L., Pironon, J., 2014. Crustal-scale fluid flow during the tectonic evolution of the Bighorn Basin (Wyoming, USA). Basin Res. 26, 403–435.
Beaudoin, N., Koehn, D., Lacombe, O., Lecouty, A., Billi, A., Aharonov, E., Parlangeau, C., 2016. Fingerprinting stress: stylolite and calcite twinning paleopiezometry reveal the complexity of progressive stress patterns during folding - the case of the Monte Nero anticline in the Apennines, Italy. Tectonics 35:1687–1712. http://dx.doi.org/10.1002/2016TC004128.
Bellani, S., Brogi, A., Lazzarotto, A., Liotta, D., Ranalli, G., 2004. Heat flow, deep temperatures and extensional structures in the Larderello geothermal field (Italy). Constraints on geothermal fluid flow. J. Volcanol. Geotherm. Res. 132, 15–29.
Berardi, G., Vignaroli, G., Billi, A., Rossetti, F., Soligo, M., Kele, S., Baykara, M.O., Bernasconi, S.M., Castorina, F., Tecce, F., Shen, C.-C., 2016. Growth of a Pleistocene giant carbonate vein and nearby thermogene travertine deposits at Semproniano, southern Tuscany, Italy: estimate of CO_2 leakage. Tectonophysics 690:219–239. http://dx.doi.org/10.1016/j.tecto.2016.04.014.
Billi, A., Tiberti, M.M., 2009. Possible causes of arc development in the Apennines, central Italy. Geol. Soc. Am. Bull. 121, 1409–1420.
Billi, A., Tiberti, M.M., Cavinato, G.P., Cosentino, D., Di Luzio, E., Keller, J.V.A., Kluth, C., Orlando, L., Parotto, M., Praturlon, A., Romanelli, M., Storti, F., Wardell, N., 2006. First results from the CROP-11 deep seismic profile, central Apennines, Italy: evidence of mid-crustal folding. J. Geol. Soc. Lond. 163, 583–586.
Bonciani, F., Callegari, I., Conti, P., Cornamusini, G., Carmignani, L., 2005. Neogene postcollisional evolution of the internal Northern Apennines: Insights from the upper Fiora and Albegna valleys (Mt. Amiata geothermal area, southern Tuscany). Boll. Soc. Geol. Ital. 3 (special issue), 103–118.
Brogi, A., 2004. Miocene extension in the inner northern Apennines: the Tuscan nappe megaboudins in the Mt. Amiata geothermal area and their influence on Neogene sedimentation. Boll. Soc. Geol. Ital. 123, 513–529.
Brogi, A., 2008. The structure of the Monte Amiata volcano-geothermal area (Northern Apennines, Italy): Neogene-Quaternary compression versus extension. Int. J. Earth Sci. 97, 677–703.
Brogi, A., 2016. Influence of syn-sedimentary faults on orogenic structures in a collisional belt: insights from the inner zone of the Northern Apennines (Italy). J. Struct. Geol. 86, 75–94.
Brogi, A., Capezzuoli, E., Liotta, D., Meccheri, M., 2015. The Tuscan Nappe structures in the Monte Amiata geothermal area (central Italy): a review. Ital. J. Geosci. 134, 219–236.
Brogi, A., Fabbrini, L., 2009. Extensional and strike-slip tectonics across the Monte Amiata–Monte Cetona transect (Northern Apennines, Italy) and seismotectonic implications. Tectonophysics 476, 195–209.
Brogi, A., Liotta, D., 2008. Highly extended terrains, lateral segmentation of the substratum, and basin development: the middle-late Miocene Radicondoli Basin (inner Northern Apennines, Italy). Tectonics 27:TC5002. http://dx.doi.org/10.1029/2007TC002188.
Browne, P.R.L., 1978. Hydrothermal alteration in active geothermal fields. Annu. Rev. Earth Planet. Sci. 6, 229–248.
Buonasorte, G., Cataldi, R., Ceccarelli, A., Costantini, A., D'Offizi, S., Lazzarotto, A., Ridolfi, A., Baldi, P., Barelli, A., Bertini, G., Bertrami, R., Calamai, A., Cameli, G., Corsi, R., D'Acquino, C., Fiordelisi, A., Gezzo, A., Lovari, F., 1988. Ricerca ed esplorazione nell'area geotermica di Torre Alfina (Lazio–Umbria). Boll. Soc. Geol. Ital. 107, 265–337.
Burnside, N.M., Shipton, Z.K., Dockrill, B., Ellam, R.M., 2013. Man-made versus natural CO_2 leakage: a 400 k.y. history of an analogue for engineered geological storage of CO_2. Geology 41, 471–474.
Buttinelli, M., Scrocca, D., De Rita, D., Quattrocchi, F., 2014. Modes of stepwise eastward migration of the northern Tyrrhenian Sea back-arc extension: evidences from the northern Latium offshore (Italy). Tectonics 32:187–206. http://dx.doi.org/10.1002/2013TC003365.
Cadoux, A., Pinti, D.L., 2009. Hybrid character and pre-eruptive events of Mt Amiata volcano (Italy) inferred from geochronological, petro-geochemical and isotopic data. J. Volcanol. Geotherm. Res. 179, 169–190.
Carmignani, L., Conti, P., Cornamusini, G., Pirro, A., 2013. Geological map of Tuscany (Italy). J. Maps 9:487–497. http://dx.doi.org/10.1080/17445647.2013.820154.
Cartwright, J.A., 2011. Diagenetically-induced shear failure of fine-grained sediments and the development of polygonal fault systems. Mar. Pet. Geol. 28, 1593–1610.
Cartwright, J.A., Dewhurst, D., 1998. Layer-bound compaction faults in fine-grained sediments. Geol. Soc. Am. Bull. 110, 1242–1257.
Cartwright, J.A., Lonergan, L., 1996. Volumetric contraction during the compaction of mudrocks: a mechanism for the development of regional-scale polygonal fault systems. Basin Res. 8, 183–193.
Chafetz, H.S., Folk, R.L., 1984. Travertines: depositional morphology and the bacterially-constructed constituents. J. Sediment. Petrol. 54, 289–316.
Chafetz, H.S., Guidry, S.A., 1999. Bacterial shrubs, crystal shrubs, and ray-crystal shrubs: bacterial vs. abiotic precipitation. Sediment. Geol. 126, 57–74.
Chafetz, H.S., Guidry, S.A., 2003. Deposition and diagenesis of Mammoth Hot Springs travertine, Yellowstone National Park, Wyoming, U.S.A. Can. J. Earth Sci. 40, 1515–1529.
Cipollari, P., Cosentino, D., 1995. Miocene unconformities in the central Apennines: geodynamic significance and sedimentary basin evolution. Tectonophysics 252, 375–389.
Claes, H., Degros, M., Soete, J., Claes, S., Kele, S., Mindszenty, A., Török, Á., El Desouky, H., Vanhaecke, F., Swennen, R., 2016. Geobody architecture, genesis and petrophysical characteristics of the Budakalasz travertines, Buda Hills (Hungary). Quat. Int. http://dx.doi.org/10.1016/j.quaint.2016.09.007.
Conti, A., Bigi, S., Cuffaro, M., Doglioni, C., Scrocca, D., Muccini, F., Cocchi, L., Ligi, M., Bortoluzzi, G., 2017. Transfer zones in an oblique back-arc basin setting: insights from the Latium-Campania segmented margin (Tyrrhenian Sea). Tectonics http://dx.doi.org/10.1002/2016TC004198.
Croci, A., Della Porta, G., Capezzuoli, E., 2016. Depositional architecture of a mixed travertine-terrigenous system in a fault-controlled continental extensional basin (Messinian, southern Tuscany, Central Italy). Sediment. Geol. 332, 13–39.
Crossey, L.J., Fischer, T.P., Patchett, P.J., Karlstrom, K.E., Hilton, D.R., Newell, D.L., Huntoon, P., Reynolds, A.C., de Leeuw, G.A.M., 2006. Dissected hydrologic system at the Grand Canyon: interaction between deeply derived fluids and plateau aquifer waters in modern springs and travertine. Geology 34, 25–28.
Crossey, L.J., Karlstrom, K.E., 2012. Travertines and travertine springs in eastern Grand Canyon: what they tell us about groundwater, paleoclimate, and incision of Grand Canyon. Geol. Soc. Am. Spec. Pap. 489, 131–143.
Crossey, L.C., Karlstrom, K.E., Dorsey, R., Pearce, J., Wan, E., Beard, L.S., Asmerom, Y., Polyak, V., Crow, R.S., Cohen, A., Bright, J., Pecha, M.E., 2015. Importance of groundwater in propagating downward integration of the 6–5 Ma Colorado River system: geochemistry of springs, travertines, and lacustrine carbonates of the Grand Canyon region over the past 12 Ma. Geosphere 11, 660–682.
Crossey, L.J., Karlstrom, K.E., Schmandt, B., Crow, R.R., Colman, D.R., Cron, B., Takacs-Vesbach, C.D., Dahm, C.N., Northup, D.E., Hilton, D.R., Ricketts, J.W., Lowry, A.R., 2016. Continental smokers couple mantle degassing and distinctive microbiology within continents. Earth Planet. Sci. Lett. 435, 22–30.
Crossey, L.J., Karlstrom, K.E., Springer, A.E., Newell, D., Hilton, D.R., Fischer, T., 2009. Degassing of mantle-derived CO_2 and He from springs in the southern Colorado Plateau region - neotectonic connections and implications for groundwater systems. Geol. Soc. Am. Bull. 121, 1034–1053.
De Filippis, L., Anzalone, E., Billi, A., Faccenna, C., Poncia, P.P., Sella, P., 2013a. The origin and growth of a recently-active fissure ridge travertine over a seismic fault, Tivoli, Italy. Geomorphology 195, 13–26.
De Filippis, L., Billi, A., 2012. Morphotectonics of fissure ridge travertines from geothermal areas of Mammoth Hot Springs (Wyoming) and Bridgeport (California). Tectonophysics 548–549, 34–38.
De Filippis, L., Faccenna, C., Billi, A., Anzalone, E., Brilli, M., Özkul, M., Soligo, M., Tuccimei, P., Villa, I.M., 2012. Growth of fissure ridge travertines from geothermal springs of Denizli basin, western Turkey. Geol. Soc. Am. Bull. 124, 1629–1645.
De Filippis, L., Faccenna, C., Billi, A., Anzalone, E., Brilli, M., Soligo, M., Tuccimei, P., 2013b. Plateau versus fissure ridge travertines from quaternary geothermal springs of Italy and Turkey: interactions and feedbacks among fluid discharge, paleoclimate, and tectonics. Earth Sci. Rev. 123, 35–52.
Dockrill, B., Shipton, Z.K., 2010. Structural controls on leakage from a natural CO_2 geologic storage site: Central Utah, U.S.A. J. Struct. Geol. 32, 1768–1782.
Eide, C.H., Schofield, N., Jerram, D.A., Howell, J.A., 2017. Basin-scale architecture of deeply emplaced sill complexes: Jameson Land, East Greenland. J. Geol. Soc. 174:23–40. http://dx.doi.org/10.1144/jgs2016-018.
Eiler, J.M., 2007. "Clumped-isotope" geochemistry - the study of naturally-occurring, multiply-substituted isotopologues. Earth Planet. Sci. Lett. 262, 309–327.
Einaudi, M.T., Hendequist, J.W., Inan, E.E., 2003. Sulfi dation state of fluids in active and extinct hydrothermal systems: transitions from porphyry to epithermal environments. In: Simmons, S.F., Graham, I. (Eds.), Volcanic, Geothermal, and Ore-Forming Fluids: Rulers and Witnesses of Processes within the Earth. Society of Economic Geologists Special Publication Vol. 10, pp. 285–313.
Enos, P., Lehrmann, D.J., Jiayong, Wei, Youyi, Yu, Jiafei, Xiao, Chaikin, D.H., Minzoni, M., Berry, A.K., Montgomery, P., 2006. Triassic evolution of the Yangtze Platform in Guizhou Province, People's Republic of China. Geol. Soc. Am. Spec. Pap. 417: 105. http://dx.doi.org/10.1130/2006.2417.
Faccenna, C., Becker, T.W., Lucente, F.P., Jolivet, L., Rossetti, F., 2001. History of subduction and back arc extension in the Central Mediterranean. Geophys. J. Int. 145, 809–820.
Faccenna, C., Mattei, M., Funiciello, R., Jolivet, L., 1997. Styles of back-arc extension in the central Mediterranean. Terra Nova 9, 126–130.
Faccenna, C., Soligo, M., Billi, A., De Filippis, L., Funiciello, R., Rossetti, C., Tuccimei, P., 2008. Late Pleistocene depositional cycles of the Lapis Tiburtinus travertine (Tivoli, Central Italy): possible influence of climate and fault activity. Glob. Planet. Chang. 63, 299–308.
Fletcher, R.C., Merino, E., 2001. Mineral growth in rocks: kinetic-rheological models of replacement, vein formation, and syntectonic crystallization. Geochim. Cosmochim. Acta 65, 3733–3748.
Frery, E., Gratier, J.-P., Ellouz-Zimmerman, N., Deschamps, P., Blamart, D., Hamelin, B., Swennen, R., 2016. Geochemical transect through a travertine mount: a detailed record of CO_2-enriched fluid leakage from late Pleistocene to present-day - Little Grand Wash fault (Utah, USA). Quat. Int. http://dx.doi.org/10.1016/j.quaint.2016.09.035.
Frery, E., Gratier, J.-P., Ellouz-Zimmerman, N., Loiselet, C., Braun, J., Deschamps, P., Blamart, D., Hamelin, B., Swennen, R., 2015. Evolution of fault permeability during episodic fluid circulation: evidence for the effects of fluid–rock interactions from travertine studies (Utah–USA). Tectonophysics 651–652, 121–137.

Gandin, A., Capezzuoli, E., 2008. Travertine versus calcareous tufa: distinctive petrologic features and related stable isotopes signature. Il Quaternario. Ital. J. Quaternary Sci. 21, 125–136.
Gandin, A., Wright, D.T., Melezhik, V., 2005. Vanished evaporites and carbonate formation in the Neoarchaean Kogelbeen and Gamohaan formations of the Campbellrand subgroup, South Africa. J. Afr. Earth Sci. 41, 1–23.
Ghosh, P., Adkins, J., Affek, H., Balta, B., Guo, W., Schauble, E.A., Schrag, D., Eiler, J.M., 2006. ^{13}C-^{18}O bonds in carbonate minerals: a new kind of paleothermometer. Geochim. Cosmochim. Acta 70, 1439–1456.
Gianelli, G., Manzella, A., Puxeddu, M., 1997. Crustal models of the geothermal areas of southern Tuscany (Italy). Tectonophysics 281, 221–239.
Giggenbach, W.F., 1992. Magma degassing and mineral deposition in hydrothermal systems along convergent plate boundaries. Econ. Geol. Bull. Soc. Econ. Geol. 87, 1927–1944.
Gratier, J.-P., Frery, E., Deschamps, P., Røyne, A., Renard, F., Dysthe, D., Ellouz-Zimmerman, N., Hamelin, B., 2012. How travertine veins grow from top to bottom and lift the rocks above them: the effect of crystallization force. Geology 40, 1015–1018.
Gresens, R.L., 1967. Composition-volume relationships of metasomatism. Chem. Geol. 2, 47–65.
Gündogan, I., Önalb, M., Depçi, T., 2005. Sedimentology, petrography and diagenesis of Eocene–Oligocene evaporites: the Tuzhisar Formation, SW Sivas Basin, Turkey. J. Asian Earth Sci. 25, 791–803.
Guo, L., Riding, R., 1994. Origin and diagenesis of Quaternary travertine shrub fabrics, Rapolano Terme, central Italy. Sedimentology 41, 499–520.
Guo, L., Riding, R., 1998. Hot-spring travertine facies and sequences, Late Pleistocene, Rapolano Terme, Italy. Sedimentology 45, 163–180.
Hammer, Ø., Dysthe, D.K., Jamtveit, B., 2007. The dynamics of travertine dams. Earth Planet. Sci. Lett. 256, 258–263.
Handford, C.R., Kendall, A.C., Prezbindowski, D.R., Dunham, J.B., Logan, B.W., 1984. Salina-margin tepees, pisoliths, and aragonite cements, Lake MacLeod, Western Australia: their significance in interpreting ancient analogs. Geology 12, 523–527.
Hilgers, C., Dilg-Gruschinski, K., Urai, J.L., 2004. Microstructural evolution of syn-taxial veins formed by advective flow. Geology 32, 261–264.
Hilgers, C., Urai, J.L., 2005. On the arrangement of solid inclusions in fibrous veins and the role of the crack-seal mechanism. J. Struct. Geol. 27, 481–494.
Hussain, M., Warren, J.K., 1989. Nodular and enterolithic gypsum: the "sabkha-tization" of Salt Flat playa, west Texas. Sediment. Geol. 64, 13–24.
Innocenti, F., Serri, G., Ferrara, G., Manetti, P., Tonarini, S., 1992. Genesis and classification of the rocks of the Tuscan magmatic province: thirty years after the Marinelli's model. Acta Vulcanol. 2, 247–265.
Jolivet, L., Faccenna, C., Goffé, B., Mattei, M., Rossetti, F., Brunet, C., Storti, F., Funiciello, R., Cadet, J.P., D'Agostino, N., Parra, T., 1998. Midcrustal shear zones in post-orogenic extension: example from the northern Tyrrhenian Sea (Italy). J. Geophys. Res. 103, 12,123–12,160.
Kampman, N., Burnside, N.M., Shipton, Z.K., Chapman, H.J., Nicholl, J.A., Ellam, R.A., Bickle, M.J., 2012. Pulses of carbon dioxide emissions from intracrustal faults following climatic warming. Nat. Geosci. 5, 352–358.
Karlstrom, K.E., Crossey, L.J., Embid, E., Crow, R., Heizler, M., Hereford, R., Beard, L.S., Ricketts, J.W., Cather, S., Kelley, S., 2017. Cenozoic incision history of the Little Colorado River: Its role in carving Grand Canyon and onset of rapid incision in the past ca. 2 Ma in the Colorado River System. Geosphere 13. http://dx.doi.org/10.1130/GES01304.1.
Karlstrom, K.E., Crossey, L.J., Hilton, D.R., Barry, P.H., 2013. Mantle ^{3}He and CO_2 degassing in carbonic and geothermal springs of Colorado and implications for neotectonics of the Rocky Mountains. Geology 41, 495–498.
Kele, S., Breitenbach, S.F.M., Capezzuoli, E., Nele Meckler, A., Ziegler, M., Millan, I.M., Kluge, T., Deák, J., Hanselmann, K., John, C.M., Yan, H., Liu, Z., Bernasconi, S.M., 2015. Temperature dependence of oxygen- and clumped isotope fractionation in carbonates: a study of travertines and tufas in the 6–95 °C temperature range. Geochim. Cosmochim. Acta 168, 172–192.
Kele, S., Demény, A., Siklósy, Z., Németh, T., Mária, T., Kovács, M.B., 2008. Chemical and stable isotope compositions of recent hot-water travertines and associated thermal waters, from Egerszalók, Hungary: depositional facies and non-equilibrium fractionations. Sediment. Geol. 211, 53–72.
Kele, S., Özkul, M., Gökgöz, A., Fórizs, I., Baykara, M.O., Alçiçek, M.C., Németh, T., 2011. Stable isotope geochemical and facies study of Pamukkale travertines: new evidences of low temperature non-equilibrium calcite–water fractionation. Sediment. Geol. 238, 191–212.
Kendall, C.G.St.C., Warren, J., 1987. A review of the origin and setting of tepees and their associated fabrics. Sedimentology 34, 1007–1027.
Laurenzi, M.A., Braschi, E., Casalini, M., Conticelli, S., 2015. New ^{40}Ar-^{39}Ar dating and revision of the geochronology of the Monte Amiata volcano, Central Italy. Ital. J. Geosci. 134, 255–265.
Lebatard, A.E., Alçiçek, M.C., Rochette, P., Khatib, S., Vialet, A., Boulbes, N., Bourlès, D.L., Demory, F., Guipert, G., Mayda, S., Titov, V.V., Vidal, L., de Lumley, H., 2014. Dating the *Homo erectus* bearing travertine from Kocabaş (Denizli, Turkey) at at least 1.1 Ma. Earth Planet. Sci. Lett. 390, 8–18.
Liotta, D., 1994. Structural features of the Radicofani Basin along the Piancastagnaio (Mt. Amiata)–S. Casciano dei Bagni (Mt. Cetona) cross section. Mem. Soc. Geol. Ital. 48, 401–408.
Liotta, D., Brogi, A., Meccheri, M., Dini, A., Bianco, C., Ruggieri, G., 2015. Coexistence of low-angle normal and high-angle strike- to oblique-slip faults during late Miocene mineralization in eastern Elba Island (Italy). Tectonophysics 660, 17–34.
Liotta, D., Ruggieri, G., Brogi, A., Fulignati, P., Dini, A., Cardini, I., 2010. Migration of geothermal fluids in extensional terrains: the ore deposits of the Boccheggiano-Montieri area (southern Tuscany, Italy). Int. J. Earth Sci. 99, 623–644.
Lokier, S., Steuber, T., 2009. Large-scale intertidal polygonal features of the Abu Dhabi coastline. Sedimentology 56, 609–621.
Malinverno, A., Ryan, W.B.F., 1986. Extension in the Tyrrhenian Sea and shortening in the Apennines as result of arc migration driven by sinking of the lithosphere. Tectonics 5, 227–254.
Manfra, L., Masi, U., Turi, B., 1976. La composizione isotopica dei travertini del Lazio. Geol. Romana 15, 127–174.
Marroni, M., Moratti, G., Costantini, A., Conticelli, S., Benvenuti, M.G., Pandolfi, L., Bonini, M., Cornamusini, G., Laurenzi, M.A., 2015. Geology of the Monte Amiata region, southern Tuscany, central Italy. Ital. J. Geosci. 134, 171–199.
Martini, I.P., Sagri, M., 1993. Tectono-sedimentary characteristics of late Miocene–Quaternary extensional basins of the Northern Apennines, Italy. Earth Sci. Rev. 34, 197–233.
McCrea, J.M., 1950. On the isotopic chemistry of carbonates and a paleotemperature scale. J. Chem. Phys. 18, 849–857.
Nappi, G., Renzulli, A., Santi, P., Gillot, P.Y., 1995. Geological evolution and geochronology of the Vulsini Volcano District (Central Italy). Boll. Soc. Geol. Ital. 114, 599–613.
Noiriel, C., Renard, F., Doan, M.L., Gratier, J.P., 2010. Intense fracturing and fracture sealing induced by mineral growth in porous rocks. Chem. Geol. 269, 197–209.
Özkul, M., Kele, S., Gökgöz, A., Shen, C.-C., Jones, B., Baykara, M.O., Fórizs, I., Németh, T., Chang, Y.-W., Alçiçek, M.C., 2013. Comparison of the quaternary travertine sites in the Denizli extensional basin based on their depositional and geochemical data. Sediment. Geol. 294, 179–204.
Pascucci, V., Costantini, A., Martini, I.P., Dringoli, R., 2006. Tectono-sedimentary analysis of a complex, extensional, Neogene basin formed on thrust-faulted, Northern Apennines hinterland: Radicofani Basin, Italy. Sediment. Geol. 183, 71–97.
Patacca, E., Sartori, R., Scandone, P., 1990. Tyrrhenian basin and Apenninic arcs: kinematic relation since late Tortonian times. Mem. Soc. Geol. Ital. 45, 425–451.
Pederson, J., Burnside, N., Shipton, Z., Rittenour, T., 2013. Rapid river incision across an inactive fault - implications for patterns of erosion and deformation in the central Colorado Plateau. Lithosphere 5, 513–520.
Pentecost, A., 2005. Travertine. Springer-Verlag, Berlin Heidelberg (445 pp.).
Petracchini, L., Antonellini, M., Billi, A., Scrocca, D., 2015. Syn-thrusting polygonal normal faults exposed in the hinge of the Cingoli anticline, northern Apennines, Italy. Front. Earth Sci. 3:67. http://dx.doi.org/10.3389/feart.2015.00067.
Piper, J.D.A., Mesci, L.B., G€ursoy, H., Tatar, O., Davies, C., 2007. Palaeomagnetic and rock magnetic properties of travertine: its potential as a recorder of geomagnetic palaeosecular variation, environmental change and earthquake activity in the Sicak Cermik geothermal field, Turkey. Phys. Earth Planet. In. 161, 50–73.
Priewisch, A., Crossey, L.J., Karlstrom, K.E., Polyak, V.J., Asmerom, Y., Nereson, A., Ricketts, J.W., 2014. U-series geochronology of large-volume Quaternary travertine deposits of the southeastern Colorado Plateau: evaluating episodicity and tectonic and paleohydrologic controls. Geosphere 10, 401–423.
Rae, A.J., Cooke, D.R., Phillips, D., Yeats, C., Ryan, C., Hermoso, D., 2003. Spatial and temporal relationships between hydrothermal alteration assemblages at the Palinpinon geothermal field, Philippines - implications for porphyry and epithermal ore deposits. In: Simmons, S.F., Graham, I. (Eds.), Volcanic, Geothermal, and Ore-Forming Fluids: Rulers and Witnesses of Processes Within the Earth: Economic Geologists Special Publication. Vol. 10, pp. 223–246.
Ricketts, J.W., Karlstrom, K.E., Priewisch, A., Crossey, L.J., Polyak, V.J., Asmerom, Y., 2014. Quaternary extension in the Rio Grande rift at elevated strain rates recorded in travertine deposits, central New Mexico. Lithosphere 6, 3–16.
Rihs, S., Condomines, M., Poidevin, J.L., 2000. Long-term behaviour of continental hydrothermal systems: U-series study of hydrothermal carbonates from the French Massif Central (Allier Valley). Geochim. Cosmochim. Acta 64, 3189–3199.
Rimondi, V., Costagliola, P., Ruggieri, G., Benvenuti, M., Boschi, C., Brogi, A., Capezzuoli, E., Morelli, G., Gasparon, M., Liotta, D., 2015. Investigating fossil hydrothermal systems by means of fluid inclusions and stable isotopes in banded travertine: an example from Castelnuovo dell'Abate (southern Tuscany, Italy). Int. J. Earth Sci. 105, 659–679.
Ring, U., Uysal, I.T., Yüce, G., Ünal-Imer, E., Italiano, F., Imer, A., Zhao, J.-X., 2016. Recent mantle degassing recorded by carbonic spring deposits along sinistral strike-slip faults, south-central Australia. Earth Planet. Sci. Lett. 454, 304–318.
Rodríguez-Berriguete, A., Alonso-Zarza, A.M., Martín-García, R., 2016. Diagenesis of continental carbonate country rocks underlying surficial travertine spring deposits. Quat. Int. http://dx.doi.org/10.1016/j.quaint.2016.09.013.
Ronchi, P., Cruciani, F., 2015. Continental carbonates as a hydrocarbon reservoir, an analog case study from the travertine of Saturnia, Italy. AAPG Bull. 99, 711–734.
Rose, A.W., Burt, D.M., 1979. Hydrothermal alteration. In: Barnes, H.L. (Ed.), Geochemistry of Hydrothermal Ore Deposits, second ed. John Wiley and Sons, New York, pp. 173–235.
Rossetti, F., Aldega, L., Tecce, F., Balsamo, F., Billi, A., Brilli, M., 2011. Fluid flow within the damage zone of the Boccheggiano extensional Fault (Larderello-Travale geothermal field, central Italy): structures, alteration, and implications for hydrothermal mineralisation in extensional settings. Geol. Mag. 148, 558–579.
Rossetti, F., Balsamo, F., Villa, I.M., Bouybaouenne, M., Faccenna, C., Funiciello, R., 2008. Pliocene–Pleistocene HT–LP metamorphism during multiple granitic intrusions in the southern branch of the Larderello geothermal field (southern Tuscany, Italy). J. Geol. Soc. Lond. 165, 247–262.
Rossetti, F., Faccenna, C., Jolivet, L., Funiciello, R., Tecce, F., Brunet, C., 1999. Syn-versus post-orogenic extension: the case study of Giglio Island (Northern Tyrrhenian Sea, Italy). Tectonophysics 304, 71–93.
Rossetti, F., Tecce, F., Billi, A., Brilli, M., 2007. Patterns of fluid flow in the contact aureole of the late Miocene Monte Capanne pluton (Elba Island, Italy): the role of structures and rheology. Contrib. Mineral. Petrol. 153, 743–760.
Schreiber, B.C., Helman, M.L., 2005. Criteria for distinguishing primary evaporite features from deformation features in sulphate evaporites. J. Sediment. Res. 75, 525–533.

Serri, G., Innocenti, F., Manetti, P., 1993. Geochemical and petrological evidence of the subduction of delaminated Adriatic continental lithosphere in the genesis of the Neogene–Quaternary magmatism in central Italy. Tectonophysics 223, 117–147.

Shanks III, W.C.P., 2012. Hydrothermal alteration in volcanogenic massive sulfide occurrence model. U.S. Geological Survey Scientific Investigations Report 2010–5070–C. 11, pp. 169–180.

Shen, C.-C., Wu, C.-C., Cheng, H., Edwards, R.L., Hsieh, Y.-T., Gallet, S., Chang, C.-C., Li, T.-Y., Lam, D.D., Kano, A., Hori, M., Spötl, C., 2012. High-precision and high resolution carbonate ^{230}Th dating by MC-ICP-MS with SEM protocols. Geochim. Cosmochim. Acta 99, 71–86.

Shipton, Z.K., Evans, J.P., Kirschner, D., Kolesar, P.T., Williams, A.P., Heath, J., 2004. Analysis of CO_2 leakage through "low-permeability" faults from natural reservoirs in the Colorado Plateau, east-Central Utah. Geol. Soc. Lond. Spec. Publ. 233, 43–59.

Simmons, S.F., Graham, I. (Eds.), 2003. Volcanic, Geothermal, and Ore-forming Fluids: Rulers and Witnesses of Processes within the Earth. Society of Economic Geologists Special Publication 10.

Sinisi, R., Petrullo, A.V., Agosta, F., Paternoster, M., Belviso, C., Grassa, F., 2016. Contrasting fault fluids along high-angle faults: a case study from southern Apennines (Italy). Tectonophysics 690:206–218. http://dx.doi.org/10.1016/j.tecto.2016.07.023.

Soete, J., Kleipool, L.M., Claes, H., Claes, S., Hamaekers, H., Kele, S., Ozkul, M., Foubert, A., Reijmer, J.J.G., Swennen, R., 2015. Acoustic properties in travertines and their relation to porosity and pore types. Mar. Pet. Geol. 59, 320–335.

Sumner, D.Y., 1997. Carbonate precipitation and oxygen stratification in late Archean seawater as deduced from facies and stratigraphy of the Gamohaan and Frisco Formations, Transvaal Supergroup, South Africa. Am. J. Sci. 297, 455–487.

Taber, S., 1916. The growth of crystals under external pressure. Am. J. Sci. 41, 532–556.

Tompkins, L.A., Rayner, M.J., Groves, D.I., Roche, M.T., 1994. Evaporites: in situ sulfur source for rhythmically banded ore in the Cadjebut Mississippi Valley-Type Zn-Pb deposit, western Australia. Econ. Geol. 89, 467–492.

Tuccimei, P., Giordano, G., Tedeschi, M., 2006. CO_2 release variations during the last 2000 years at the Colli Albani volcano (Roma, Italy) from speleothems studies. Earth Planet. Sci. Lett. 243, 449–462.

Ünal-İmer, E., Uysal, T., Zhao, J.-X.d., Işik, V., Shulmeister, J., İmer, A., Feng, Y.-X., 2016. CO_2 outburst events in relation to seismicity: constraints from microscale geochronology, geochemistry of late Quaternary vein carbonates, SW Turkey. Geochim. Cosmochim. Acta 187, 21–40.

Uysal, I.T., Feng, Y., Zhao, J.X., Altunel, E., Weatherley, D., Karabacak, V., Cengiz, O., Golding, S.D., Lawrence, M.G., Collerson, K.D., 2007. U-series dating and geochemical tracing of late Quaternary travertine in co-seismic fissures. Earth Planet. Sci. Lett. 257, 450–462.

Uysal, I.T., Feng, Y., Zhao, J.X., Isik, V., Nuriel, P., Golding, S.D., 2009. Hydrotermal CO_2 degassing in seismically active zones during the late Quaternary. Chem. Geol. 265, 442–454.

Vignaroli, G., Aldega, L., Balsamo, F., Billi, A., De Benedetti, A.A., De Filippis, L., Giordano, G., Rossetti, F., 2015. A way to hydrothermal paroxysm, Colli Albani Volcano, Italy. Geol. Soc. Am. Bull. 127, 672–687.

Vignaroli, G., Berardi, G., Billi, A., Kele, S., Rossetti, F., Soligo, M., Bernasconi, S.M., 2016. Tectonics, hydrothermalism, and paleoclimate recorded by Quaternary travertines and their spatio-temporal distribution in the Albegna basin, central Italy: insights on Tyrrhenian margin neotectonics. Lithosphere 8:335–358. http://dx.doi.org/10.1130/L507.1.

Vignaroli, G., Pinton, A., De Benedetti, A.A., Giordano, G., Rossetti, F., Soligo, M., Berardi, G., 2013. Structural compartmentalisation of a geothermal system, the Torre Alfina field (central Italy). Tectonophysics 608, 482–498.

Wang, X., Auler, A.S., Edwards, R.L., Cheng, H., Cristalli, P.S., Smart, P.L., Richards, D.A., Shen, C.-C., 2004. Wet periods in northeastern Brazil over the past 210 kyr linked to distant climate anomalies. Nature 432, 740–743.

Wang, H., Yan, H., Liu, Z., 2014. Contrasts in variations of the carbon and oxygen isotopic composition of travertines formed in pools and a ramp stream at Huanglong Ravine, China: implications for paleoclimatic interpretations. Geochim. Cosmochim. Acta 125, 34–48.

Watts, N.L., 1978. Displacive calcite: evidence from recent and ancient calcretes. Geology 6, 699–703.

West, I.M., 1965. Macrocell structure and enterolithic veins in British Purbeck gypsum and anhydrite. Proc. Yorks. Geol. Soc. 35, 47–58.

Weyl, P.K., 1959. Pressure solution and the force of crystallization: a phenomenological theory. J. Geophys. Res. 64, 2001–2025.

Wiltschko, D.V., Morse, J.W., 2001. Crystallization pressure versus "crack seal" as the mechanism for banded veins. Geology 29, 79–82.

Zanchi, A., Tozzi, M., 1987. Evoluzione paleogeografica e strutturale recente del bacino del fiume Albegna (Toscana meridionale). Geol. Romana 26, 305–325.